

# MODELLING STRONG DISCONTINUITIES IN SOLID MECHANICS VIA STRAIN SOFTENING CONSTITUTIVE EQUATIONS. PART 1: FUNDAMENTALS

J. OLIVER

*E.T.S. d'Enginyers de Camins, Canals i Ports, Technical University of Catalonia, Gran Capità s/n. Mòdul C-1, 08034 Barcelona, Spain*

## SUMMARY

The paper addresses some fundamental aspects about the use of standard constitutive equations to model strong discontinuities (cracks, shear bands, slip lines, etc.) in solid mechanics analyzes. The strong discontinuity analysis is introduced as a basic tool to derive a general framework, in which different families of constitutive equations can be considered, that allows to extract some outstanding aspects of the intended analysis. In particular, a link between continuum and discrete approaches to the strain localization phenomena is obtained. Applications to standard continuum damage and elastoplastic constitutive equations are presented. Relevant aspects to be considered in the numerical simulation of the problem (tackled in Part 2 of the work) are also presented.

KEY WORDS: strong discontinuity analysis; localization; damage; plasticity; strain softening

## 1. INTRODUCTION

Solid mechanics analyzes are generally conducted in the context of the *strict* Continuum Mechanics where continuity of the displacement field is postulated. However, in many engineering problems consideration of jumps in the displacement field is essential: cracks in rocks or concrete, slip lines in soils and shear bands in metals (when observed from a macroscopic point of view), have necessarily to be regarded when the aim of the analysis is to approach limit situations close to intensive damage or collapse. From now on we will understand by *strong discontinuities* these jumps in the displacement field appearing at a certain time, in general unknown before the analysis, of the loading history and developing across paths of the solid which are material (fixed) surfaces. They have to be distinguished from *weak discontinuities* that correspond to jumps in the strain field (the displacement remaining continuous) which develop along moving surfaces.<sup>1</sup>

The presently available methodologies for the numerical simulation of strong discontinuities could be classified in to two large families: discrete and continuum approaches.

*Discrete approaches*<sup>2–4</sup> are close to classical non-linear Fracture Mechanics and consider specific traction vector vs. jump constitutive equations to characterize the cohesive behaviour at the discontinuity interface, whereas for the continuous part of the body regular stress–strain constitutive equations are used. In addition, appropriate criteria for the determination of the initiation and propagation of the discontinuity have to be considered.

On the contrary, in *continuum* approaches the complete solid is regarded from a Continuum Mechanics environment: the concept of strain is defined not only in the continuous part of the

body, but also at the discontinuous interface and, therefore, standard stress–strain constitutive equations can be considered everywhere. Then, the discontinuity is modelled via two basic ingredients: (a) an implicit (sometimes not recognized) regularization of the discontinuous displacement field which is approximated by means of high displacement gradients (strain localization) in a band whose width is characterized by the so-called *characteristic length* which is taken as a material property<sup>5</sup> or, some times, as a numerical parameter,<sup>6</sup> and (b) special constitutive equations whose particular structure leads to the wellposedness of the partial differential equations governing the problem and allowing the strain localization to appear. In the recent years, much effort has been devoted to develop different approaches belonging to this family: the *smearred* crack methods using (regularized) local constitutive equations exhibiting strain softening<sup>7,8</sup>, non-local constitutive equations,<sup>9</sup> Cosserat continuum, gradient plasticity,<sup>10</sup> viscoplasticity<sup>11</sup> (or in general viscoregularized constitutive equations) could be mentioned as typical examples.

In this work the concept of *strong discontinuity analysis* already introduced in previous works<sup>12–17</sup> is used to bridge from continuum to discrete approaches. The aim of the analysis is to identify, in a general framework independent of the numerical method of simulation, the key qualitative features that make the standard stress–strain constitutive equations consistent with the appearance of strong discontinuities. In particular, the analysis provides a *discrete* (i.e. stress vs. displacement-jump) constitutive equation at the discontinuity path which is consistent with the chosen *continuum* (stress–strain) constitutive equation. At this point it is possible to chose for modelling purposes between:

- (a) a *continuum framework*: by regularizing the discontinuous displacement field (in such a way that the strains are bounded everywhere) and then using standard stress–strain constitutive equations;
- (b) a *discrete framework*: by using the derived set of discrete (stress vs. displacement-jump) constitutive equations to describe the cohesive behaviour of the discontinuity path.

In order to state the generality of the analysis, it is driven for two different families of constitutive equations: continuum damage and elastoplasticity models. Then, it is shown that, in spite of the differences between these constitutive equations, a common methodology of analysis can be applied in both cases which can be easily extended to other constitutive equations.

On the other hand, a set of relevant points emerging from the strong discontinuity analysis can be directly used in the design of specific finite elements for capturing strong discontinuities, in such a way that many unsuitable features of classical approaches (mesh-size and mesh-alignment dependencies, intrinsic limitations on the element size, etc.) can be automatically removed. This topic will be addressed in a second part of this work.

## 2. KINEMATICS: DISCONTINUOUS DISPLACEMENT FIELDS

Let us consider the reference configuration  $\Omega$  of a body exhibiting strong discontinuities along a discontinuity path  $\mathcal{S}$  which is a material surface (i.e. fixed at the reference configuration) with a unit normal vector  $\mathbf{n}$  (see Figure 1).

For practical purposes we can assume that  $\mathcal{S}$  splits the body into two parts\*  $\Omega^+$  and  $\Omega^-$  in such a way that a Heaviside function  $H_{\mathcal{S}}(\mathbf{x})$  ( $\mathbf{x}$  being the material co-ordinates of the particles,

\*Strictly speaking,  $\mathcal{S}$  could be thought as the discontinuity path (not necessarily splitting the body) plus *any* extension splitting the body and allowing  $\Omega^+$  and  $\Omega^-$  to be defined

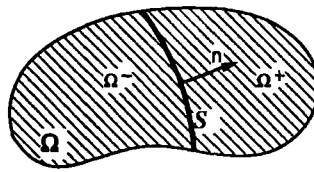


Figure 1. Definition of the discontinuity path

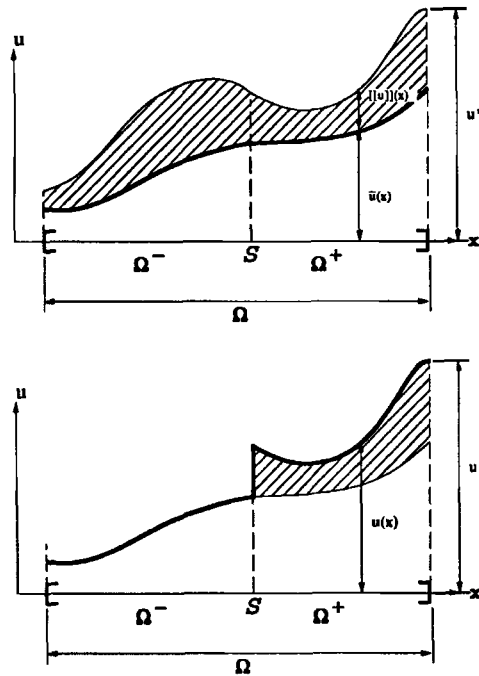


Figure 2. Kinematic decomposition of the displacement field satisfying the essential boundary condition  $u = u^*$

$H_{\mathcal{S}}(\mathbf{x}) = 1 \forall \mathbf{x} \in \Omega^+$  and  $H_{\mathcal{S}}(\mathbf{x}) = 0 \forall \mathbf{x} \in \Omega^-$  can be defined on  $\Omega$ . The most general expression of a displacement field exhibiting strong discontinuities in  $\mathcal{S}$  can be written as

$$\mathbf{u}(\mathbf{x}, t) = \bar{\mathbf{u}}(\mathbf{x}, t) + H_{\mathcal{S}}(\mathbf{x})[[\mathbf{u}]](\mathbf{x}, t) \tag{1}$$

where  $t$  refers to time,  $\bar{\mathbf{u}}(\mathbf{x}, t)$  is the regular part of the displacement field and  $[[\mathbf{u}]](\mathbf{x}, t)$  is a displacement jump function which is continuous everywhere in the body.<sup>†</sup> In Figure 2 the displacement decomposition (1) is depicted for 1-D cases.

From (1) a jump  $[[\mathbf{u}]]_{\mathcal{S}}$  of the field  $\mathbf{u}$  appears in  $\mathcal{S}$  as

$$[[\mathbf{u}]](\mathbf{x}, t)|_{\mathbf{x} \in \mathcal{S}} = [[\mathbf{u}]]_{\mathcal{S}} \tag{2}$$

<sup>†</sup> The discontinuity of the resulting displacement field in equation (1) is then achieved through the jump of the Heaviside function  $H_{\mathcal{S}}$  across  $\mathcal{S}$

The corresponding strain field can be obtained by computing the symmetric part of the gradient of the displacement field of (1), this leading to

$$\begin{aligned}\boldsymbol{\varepsilon} &= (\nabla \mathbf{u})^S = \underbrace{(\nabla \bar{\mathbf{u}})^S + H_{\mathcal{S}} (\nabla \llbracket \mathbf{u} \rrbracket)^S}_{\bar{\boldsymbol{\varepsilon}}} + \delta_{\mathcal{S}} (\llbracket \mathbf{u} \rrbracket \otimes \mathbf{n})^S \\ &= \bar{\boldsymbol{\varepsilon}} + \delta_{\mathcal{S}} (\llbracket \mathbf{u} \rrbracket \otimes \mathbf{n})^S\end{aligned}\quad (3)$$

where superscript  $(\cdot)^S$  means the symmetric part of  $(\cdot)$  and  $\delta_{\mathcal{S}}$  is the Dirac's line delta-function along  $\mathcal{S}$ , satisfying

$$\int_{\Omega} \delta_{\mathcal{S}} \varphi_0 \, d\Omega = \int_{\mathcal{S}} \varphi_0 \, d\Gamma \quad \forall \varphi_0 \in C_0^{\infty}(\Omega) \quad (4)$$

In (3) the terms  $(\nabla \bar{\mathbf{u}})^S$  and  $H_{\mathcal{S}}(\nabla \llbracket \mathbf{u} \rrbracket)^S$  have been collected in the term  $\bar{\boldsymbol{\varepsilon}}$ , that is, the regular part of the strain field exhibiting, at most, *bounded* discontinuities across  $\mathcal{S}$ . The unbounded character of the term  $\delta_{\mathcal{S}}(\llbracket \mathbf{u} \rrbracket \otimes \mathbf{n})^S$  emerges from the gradient of the Heaviside function appearing in equation (1).

### 3. STRONG DISCONTINUITY ANALYSIS

The concept of strong discontinuity analysis applies to any standard constitutive equation. The goal of the analysis is to extract the key qualitative features that make such a constitutive equation *consistent* with the appearance of strong discontinuities and, thus, with the unbounded strain fields (3). For this purpose the following set of requirements is imposed on the stress field provided by the constitutive equation:

- (I) The stress field is *bounded* everywhere in  $\Omega$ .
- (II) The *traction vector is continuous* across  $S$  at any time of the analysis.
- (III) At any point  $P$  of the discontinuity surface  $S$ , the normal  $\mathbf{n}$  is provided by the stress field at the *initiation time* (the time at which the discontinuity initiates at the considered point  $P$ ).

Justification of condition (I) comes from the non-physical sense of unbounded stresses (even at the discontinuity path  $\mathcal{S}$ , where the strains are unbounded according to (3)). Condition (II) emerges from the equilibrium conditions across the discontinuity path or, more formally, from the balance laws (see Reference [14] for more details). Finally, condition (III) establishes the material surface character of  $S$ , thus precluding any evolution of  $\mathbf{n}$  beyond the initiation time.

In the next sections two different constitutive equations, belonging to the families of *continuum damage* and *plasticity* models are analysed from the preceding point of view.

### 4. STRONG DISCONTINUITY ANALYSIS OF DAMAGE MODELS

#### 4.1. An isotropic continuum damage model

Let us consider the family of constitutive equations defined by<sup>7</sup>

$$\Psi = (1 - d)\Psi_0, \quad \Psi_0 = \frac{1}{2} \boldsymbol{\varepsilon} : \mathbf{C} : \boldsymbol{\varepsilon} \quad (5)$$

$$\boldsymbol{\sigma} = \frac{\partial \Psi}{\partial \boldsymbol{\varepsilon}} = (1 - d) \mathbf{C} : \boldsymbol{\varepsilon} \quad (6)$$

where  $\Psi$  is the Helmholtz's free energy,  $\mathbf{C}$  the elastic constitutive tensor,  $\boldsymbol{\sigma}$  the stress tensor and  $d$  the scalar damage variable ( $0 \leq d \leq 1$ ). The value of the internal variable  $d$  is given by

the corresponding damage condition and evolution laws. After some specialization<sup>7</sup> the damage variable evolution can be integrated in close form at time  $t$  giving

$$\begin{aligned} d_t &= G(r_t) \\ r_t &= \max_{s \in (-\infty, t)} \{r_0, \tau_s^e\} \end{aligned} \tag{7}$$

In (7)  $\tau^e$  is an appropriate norm of the strains described below,  $r_0$  is an initial threshold value and  $G(\cdot)$  is a non-decreasing scalar function such that  $G(r_0)=0$ ,  $G(\infty) \leq 1$  and  $G'(\mu) \geq 0 \forall \mu \in [r_0, \infty)$ . The variable  $r_t$  describes, at time  $t$ , the size of the elastic domain in the strain space  $E_\varepsilon$  defined as

$$E_\varepsilon := \{\varepsilon \mid \tau^e \leq r_t\} \tag{8}$$

Under such conditions it is straightforward to check that both  $d$  and  $r$  always increase along time so that

$$\begin{aligned} \dot{d} &\geq 0 \\ \dot{r} &\geq 0 \end{aligned} \tag{9}$$

where  $\dot{d} = 0$  for unloading and elastic loading, whereas  $\dot{d} > 0$  corresponds to inelastic loading.

Finally, from (5) and (6) the dissipation  $\mathcal{D}$  can be computed as

$$\mathcal{D} = -\dot{\Psi} + \sigma : \dot{\varepsilon} = \dot{d} \Psi_0 \geq 0 \tag{10}$$

By specialization of the function  $G(\cdot)$  and the norm  $\tau^e$  in (7) different qualitative behaviours can be modelled.<sup>7</sup> Some possible choices are given in Appendix I. For the sake of simplicity we will consider in the following a linear strain hardening-softening law with symmetric tension-compression behaviour defined by

$$\tau^e = \sqrt{\varepsilon : \mathbf{C} : \varepsilon} \tag{11}$$

$$d = G(r) = \begin{cases} 0, & r < r_0 = \sigma_u / \sqrt{E} \\ \frac{1}{1 + \mathcal{H}} \left(1 - \frac{r_0}{r}\right), & r_0 < r < r_{\max} = -\frac{1}{\mathcal{H}} r_0 \quad (\mathcal{H} < 0) \\ 1, & r_{\max} < r \end{cases} \tag{12}$$

In (12)  $\mathcal{H}$  plays the role of softening parameter,  $\sigma_u$  is the uniaxial peak stress and  $E$  is the Young modulus. The corresponding uniaxial stress-strain law is depicted in Figure 3.

Observe from (6) and (11) that a new norm  $\tau^\sigma$  in the stress domain could have been defined as

$$\tau^\sigma = \sqrt{\sigma : \mathbf{C}^{-1} : \sigma} = (1 - d) \sqrt{\varepsilon : \mathbf{C} : \varepsilon} = (1 - d) \tau^e \tag{13}$$

For the purposes of this analysis the norm  $\tau^\sigma$  is more suitable than  $\tau^e$ , so that in the following the model will be described in terms of  $\tau^\sigma$  keeping in mind that both norms are related through (13).

After some algebraic computations, the corresponding incremental stress-strain law can be computed as

$$\dot{\sigma} = \mathcal{C}^d : \dot{\varepsilon} \tag{14}$$

where  $\mathcal{C}^d$  is the tangent constitutive operator computed as

$$\begin{aligned} \dot{d} = 0 \text{ (unloading)} : \mathcal{C}^d &= (1 - d) \mathbf{C} \\ \dot{d} \neq 0 \text{ (loading)} : \mathcal{C}^d &= (1 - d) \left[ \mathbf{C} - \frac{1}{(1 + \mathcal{H})} \frac{\tau_0}{(\tau^\sigma)^3} \sigma \otimes \sigma \right] \end{aligned} \tag{15}$$

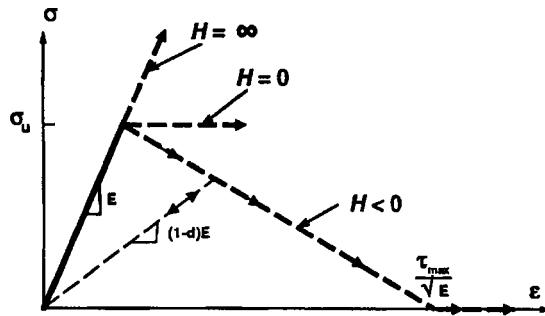


Figure 3. Damage model: uniaxial stress–strain law

Finally, the dissipation can be rewritten in a suitable form as

$$\mathcal{D} = \frac{1}{2}(\tau^\sigma)^2 \frac{\partial}{\partial t} \left( \frac{d}{1-d} \right) \geq 0 \tag{16}$$

where the term  $d/(1 - d)$  can be expressed, under loading conditions, as

$$\frac{d}{1-d} = \frac{1}{\mathcal{H}} g \tag{17}$$

$$g(\sigma) = 1 - \frac{r_0}{\tau^\sigma(\sigma)} \tag{18}$$

*Remark 1.* Observe from (13) and (18) that if the stresses are bounded (and different from zero) so is  $g$ . Also observe that negative values of the hardening-softening parameter ( $\mathcal{H} < 0 \implies$  strain softening) keep the stresses bounded for any (even unbounded) value of the strain field (see Figure 3 for 1-D cases). These facts will be conveniently exploited in next sections.

4.2. Condition (I): Stress boundedness

The constitutive equation (6) can be conveniently rephrased as

$$\left( 1 + \frac{d}{1-d} \right) \sigma = \mathbf{C} : \varepsilon \tag{19}$$

and by substitution of the strain field (3) into (19), we arrive at

$$\underbrace{\sigma}_{\text{bounded}} + \frac{d}{1-d} \sigma = \underbrace{\mathbf{C} : \bar{\varepsilon}}_{\text{bounded}} + \underbrace{\delta_{\mathcal{D}} \mathbf{C} : ([[\mathbf{u}]]_{\nu} \otimes \mathbf{n})^S}_{\text{unbounded}} \tag{20}$$

Inspection of (20) states that if we impose the stress field to be bounded, then the first term of the left-hand side is bounded and so is the first term on the right-hand side due to the bounded nature of  $\bar{\varepsilon}$  (see equation (3)). Moreover, as we are looking for discontinuous solutions of the problem, then  $[[\mathbf{u}]]_{\nu} \neq 0$  and, thus, the last term of (20) is unbounded. Finally, in order that the whole equation has a mathematical sense, this unbounded term has to be cancelled by some additional unbounded term in (20) including a delta function (the only available candidate is  $d/(1 - d)$ ). Since

inspection of the term  $d/(1 - d)$ , in (17) and (18), states that  $g$  is bounded<sup>‡</sup> (see Remark 1) the only feasible possibility is

$$\frac{1}{\mathcal{H}} = \underbrace{\delta_{\mathcal{S}} \frac{1}{\mathcal{H}}}_{\text{unbounded}} + \underbrace{\frac{1}{\mathcal{H}^*}}_{\text{regular}} \tag{21}$$

For the sake of simplicity we will restrict in the following to the particular case  $1/\mathcal{H}^* = 0$  (the analysis could be continued for the general case but no additional insight in the problem is gained), so that

$$\frac{1}{\mathcal{H}} = \delta_{\mathcal{S}} \frac{1}{\mathcal{H}} \tag{22}$$

Equation (22) states a crucial consequence of the stress boundedness requirement, that is: the *distributional character* of the softening parameter  $\mathcal{H}$  whose inverse has the structure of a delta function with an intensity given by  $1/\mathcal{H}$ . The parameter  $\mathcal{H}$  will be termed from now on *the intrinsic softening parameter*.

By substitution of (22) into (17) and then in (20) we arrive at

$$\underbrace{[\boldsymbol{\sigma} - \mathbf{C} : \bar{\boldsymbol{\varepsilon}}]}_{=0 \text{ in } \Omega \setminus \mathcal{S}} = \delta_{\mathcal{S}} \underbrace{\left[ \mathbf{C} : ([\mathbf{u}] \otimes \mathbf{n})^S - \frac{1}{\mathcal{H}} g \boldsymbol{\sigma} \right]}_{=0 \text{ in } \mathcal{S}} \tag{23}$$

In order that (23) has a mathematical sense the underbraced terms on the left and the right-hand sides have to cancel at the continuous ( $\Omega \setminus \mathcal{S}$ ) and discontinuous ( $\mathcal{S}$ ) parts of the body, respectively. Thus, the corresponding stress fields emerge from (23) as:

$$\boldsymbol{\sigma}_{\Omega \setminus \mathcal{S}} = \mathbf{C} : \bar{\boldsymbol{\varepsilon}} \tag{24}$$

$$\boldsymbol{\sigma}_{\mathcal{S}} = \frac{\bar{\mathcal{H}}}{g(\boldsymbol{\sigma}_{\mathcal{S}})} \mathbf{C} : ([\mathbf{u}]_{\mathcal{S}} \otimes \mathbf{n})^S \tag{25}$$

*Remark 2.* Equation (24) states the elastic behaviour in the continuous part of the body in terms of the regular part of the strains  $\bar{\boldsymbol{\varepsilon}}$ . An inelastic behaviour could have been considered by using the whole of equation (21) instead of the simplified one (22).

*Remark 3.* Equation (25) provides a discrete non-linear stress-jump constitutive equation at the interface  $\mathcal{S}$  (discontinuity path) which allows *the determination of the complete stress tensor on  $\mathcal{S}$  in terms of the jump  $[\mathbf{u}]_{\mathcal{S}}$  and the normal  $\mathbf{n}$* . So, unlike what is usual for constitutive equations at discontinuous interfaces, not only the traction vector is involved. Moreover, this *discrete* constitutive equation is *consistent* (emerges naturally from the stress boundedness requirement) with the original continuous constitutive equation described in Section 4.1. In particular, (25) allow the determination of the jump in terms of the stresses at the interface. Choosing an appropriate orthogonal basis formed by the unit vectors  $\mathbf{n}, \mathbf{p}, \mathbf{q}$  ( $\mathbf{n} \cdot \mathbf{p} = \mathbf{n} \cdot \mathbf{q} = \mathbf{p} \cdot \mathbf{q} = 0$ ), the components of

<sup>‡</sup> The case  $\boldsymbol{\sigma} = \mathbf{0}$  also applies here since  $g\boldsymbol{\sigma}$  can be shown to be bounded in this case

$[[\mathbf{u}]]_{\mathcal{S}}$  and  $\boldsymbol{\sigma}_{\mathcal{S}}$  on this basis are related by (see Appendix II for details)

$$\begin{bmatrix} [[\mathbf{u}]]_n \\ [[\mathbf{u}]]_p \\ [[\mathbf{u}]]_q \end{bmatrix}_{\mathcal{S}} = \frac{g_{\mathcal{S}}}{\mathcal{H}} \frac{1}{E} \begin{bmatrix} \frac{(1+\nu)(1-2\nu)}{1-\nu} & 0 & 0 \\ 0 & 1+\nu & 0 \\ 0 & 0 & 1+\nu \end{bmatrix} \begin{bmatrix} \sigma_{nn} \\ \sigma_{np} \\ \sigma_{nq} \end{bmatrix}_{\mathcal{S}} \tag{26}$$

$$\sigma_{pp_{\mathcal{S}}} = \sigma_{qq_{\mathcal{S}}} = \frac{\nu}{1-\nu} \sigma_{nn_{\mathcal{S}}}, \quad \sigma_{pq_{\mathcal{S}}} = 0 \tag{27}$$

Observe that the appearance of the term  $g_{\mathcal{S}} = g(\boldsymbol{\sigma}_{\mathcal{S}})$  in (26) precludes, in general, a linear dependence of the jump with respect to the traction vector  $\boldsymbol{\sigma}_{\mathcal{S}} \cdot \mathbf{n} = [\sigma_{nn}, \sigma_{np}, \sigma_{nq}]_{\mathcal{S}}^T$  and involves all the components of the stress tensor in the resolved jump.<sup>§</sup>

*Remark 4.* Equation (20) precludes the appearance of the jump in the initial elastic domain ( $d = 0$ ). In fact, in this case (20) reads

$$\underbrace{\boldsymbol{\sigma}}_{\text{bounded}} = \underbrace{\mathbf{C} : \bar{\boldsymbol{\epsilon}}}_{\text{bounded}} + \underbrace{\delta_{\mathcal{S}} \mathbf{C} : ([[ \mathbf{u} ] ]_{\mathcal{S}} \otimes \mathbf{n})^S}_{\text{unbounded}} \tag{28}$$

and the stress boundedness requirement forces the unbounded term of (28) to drop so that  $[[\mathbf{u}]]_{\mathcal{S}} = 0$ .

*Remark 5.* Observe that the arguments employed to obtain (25) can be reversed in the following sense: if (a) the distributional character of the hardening-softening parameter, equation (22), is enforced (consequently the elastic behaviour defined by (24) is considered in  $(\Omega \setminus \mathcal{S})$  and (b) strain-softening is considered for the constitutive behaviour for  $\mathcal{S}$  ( $\mathcal{H} < 0$ ), then the stresses are bounded both in  $\Omega \setminus \mathcal{S}$  (since  $\bar{\boldsymbol{\epsilon}}$  is bounded in (24)) and in  $\mathcal{S}$  (see Remark 1). Therefore, (25) is automatically fulfilled from the imposition of the standard constitutive equation (6) through consistency of (23). This argument is crucial to avoid the explicit imposition of (25), which are specific (and sometimes difficult to derive) of the considered constitutive equation, and it will be exploited for the numerical simulation of the problem.

### 4.3. Condition (II): Traction vector continuity

Once the stress field is determined in terms of the displacement jump by (25), the next step is the determination of the jump itself. The necessary set of equations is obtained by stating that the traction vector at the continuous part of the body  $\Omega \setminus \mathcal{S}$  in the neighbourhood<sup>¶</sup> of  $\mathcal{S}$  equals the traction vector at the discontinuity surface, i.e.

$$\boldsymbol{\sigma}_{\Omega \setminus \mathcal{S}} \Big|_{\mathbf{x} \in \mathcal{S}} \cdot \mathbf{n} = \boldsymbol{\sigma}_{\mathcal{S}} \cdot \mathbf{n} \tag{29}$$

<sup>§</sup>For unloading processes ( $d = 0$ ) then  $\dot{g}_{\mathcal{S}} = 0$  according to (17) so, in this case, (26) are incrementally linear in the traction vector

<sup>¶</sup>No distinction is made between the traction vector at the positive ( $\Omega^+$ ) or negative ( $\Omega^-$ ) neighbourhoods of  $\mathcal{S}$ , which are assumed to be the same from the balance laws<sup>14</sup>



and from (24) and (25),

$$\mathbf{n} \cdot \mathbf{C} : \bar{\boldsymbol{\varepsilon}} = \frac{\bar{\mathcal{H}}}{g_\nu} \mathbf{n} \cdot \mathbf{C} : ([[\mathbf{u}]]_\nu \otimes \mathbf{n})^S = \frac{\bar{\mathcal{H}}}{g_\nu} \mathbf{n} \cdot \mathbf{C} \cdot \mathbf{n} \cdot [[\mathbf{u}]]_\nu \quad (30)$$

Finally, solving for the jump in (30) one arrives at

$$[[\mathbf{u}]]_\nu = \frac{g(\boldsymbol{\sigma}_\nu([[\mathbf{u}]]_\nu, \mathbf{n}))}{\bar{\mathcal{H}}} \mathbf{Q}^{e-1} \cdot \mathbf{n} \cdot \mathbf{C} : \bar{\boldsymbol{\varepsilon}}_\nu \quad (31)$$

$$\mathbf{Q}^e = \mathbf{n} \cdot \mathbf{C} \cdot \mathbf{n}$$

where  $\mathbf{Q}^e$  is the elastic acoustic tensor<sup>18</sup>.

*Remark 6.* Equation (31), in view of (25), provides the jump  $[[\mathbf{u}]]_\nu$  in terms of the regular part of the strains  $\bar{\boldsymbol{\varepsilon}}_\nu$  and the normal  $\mathbf{n}$ . Again, it is emphasized that (31), which is dependent on the considered type of constitutive equation, need not to be explicitly derived for simulation purposes. The relevant fact is that the traction vector continuity requirement of (29) provides the set of equations which determines the jump.

#### 4.4. Condition (III): Identification of the normal

Let us consider any material point  $P$  at the discontinuity surface  $\mathcal{S}$  and let  $t_0$  be the time in which the discontinuity initiates at  $P$  (the initiation time) characterized by

$$[[\mathbf{u}]](\mathbf{x}_p, t_0) = [[\mathbf{u}]]_\nu^0 = 0 \quad (32)$$

$$[[\dot{\mathbf{u}}]](\mathbf{x}_p, t_0) = [[\dot{\mathbf{u}}]]_\nu^0 \neq 0$$

Equation (25) can be rewritten as

$$g_\nu \boldsymbol{\sigma}_\nu = \bar{\mathcal{H}} \mathbf{C} : ([[\mathbf{u}]]_\nu \otimes \mathbf{n})^S \quad (33)$$

and taking time derivatives in (33) we get

$$\dot{g}_\nu \boldsymbol{\sigma}_\nu + g_\nu \dot{\boldsymbol{\sigma}}_\nu = \bar{\mathcal{H}} \mathbf{C} : ([[\dot{\mathbf{u}}]]_\nu \otimes \mathbf{n})^S \quad (34)$$

where the character of material surface of  $\mathcal{S}$  has been considered ( $\dot{\mathbf{n}} = 0$ ). Equation (34) holds at any time and in particular at the initiation time  $t_0$ , where according to (32)<sub>1</sub>  $[[\mathbf{u}]]_\nu^0 = 0$ , so that from (33)  $g_\nu^0 = 0$  and (34) leads to

$$\dot{g}_\nu^0 \boldsymbol{\sigma}_\nu^0 = \bar{\mathcal{H}} \mathbf{C} : ([[\dot{\mathbf{u}}]]_\nu^0 \otimes \mathbf{n})^S \quad (35)$$

On the other hand, at the initiation time  $[[\mathbf{u}]]_\nu^0 = 0$  and  $g_\nu^0 = 0$  so that  $\boldsymbol{\varepsilon}_\nu^0 = \bar{\boldsymbol{\varepsilon}}_\nu^0$  and  $d^0 = 0$  (see (3) and (17), respectively) and finally one can write

$$\boldsymbol{\sigma}_\nu^0 = \mathbf{C} : \bar{\boldsymbol{\varepsilon}}_\nu^0 \quad (36)$$

Substituting (36) into (35) we arrive at

$$\mathbf{C} : ([[\dot{\mathbf{u}}]]_\nu^0 \otimes \mathbf{n})^S = \frac{\dot{g}_\nu^0}{\bar{\mathcal{H}}} \boldsymbol{\sigma}_\nu^0 = \frac{\dot{g}_\nu^0}{\bar{\mathcal{H}}} \mathbf{C} : \bar{\boldsymbol{\varepsilon}}_\nu^0 \quad (37)$$

and premultiplying both sides of (37) times  $\mathbf{C}^{-1}$ :

$$([\dot{\mathbf{u}}]_{\mathcal{S}}^0 \otimes \mathbf{n})^S = \frac{\dot{g}_{\mathcal{S}}^0}{\mathcal{H}} \bar{\boldsymbol{\varepsilon}}_{\mathcal{S}}^0 \tag{38}$$

Equations (38) provide a set of equations for the determination of both  $[\dot{\mathbf{u}}]_{\mathcal{S}}^0$  and  $\mathbf{n}$ . In particular, the normal  $\mathbf{n}$  can be determined by taking advantage of the structure of the right-hand side of (38). In fact, pre- and post-multiplying both sides of the equation by *any* vector  $\mathbf{t}$  orthogonal to  $\mathbf{n}$ , the left-hand side of (38) cancels so

$$\mathbf{t} \cdot ([\dot{\mathbf{u}}]_{\mathcal{S}}^0 \otimes \mathbf{n})^S \cdot \mathbf{t} = 0 = \frac{\dot{g}_{\mathcal{S}}^0}{\mathcal{H}} \mathbf{t} \cdot \bar{\boldsymbol{\varepsilon}}_{\mathcal{S}}^0 \cdot \mathbf{t} \tag{39}$$

so that

$$\mathbf{t} \cdot \bar{\boldsymbol{\varepsilon}}_{\mathcal{S}}^0 \cdot \mathbf{t} = 0 \quad \forall \mathbf{t} \mid \mathbf{t} \cdot \mathbf{n} = 0 \tag{40}$$

*Remark 7.* Equation (40) is sufficient for the determination of the normal  $\mathbf{n}$  at any point of  $\mathcal{S}$  in terms of the regular (bounded) part of the strains  $\bar{\boldsymbol{\varepsilon}}_{\mathcal{S}}^0$  at the initiation time. In particular, for 2-D cases, since the normal and tangent vectors can be defined by an inclination angle  $\theta$  with respect to an orthogonal basis  $\hat{\mathbf{e}}_1$  and  $\hat{\mathbf{e}}_2$  as

$$\begin{aligned} \mathbf{n} &= \cos \theta \hat{\mathbf{e}}_1 + \sin \theta \hat{\mathbf{e}}_2 \\ \mathbf{t} &= -\sin \theta \hat{\mathbf{e}}_1 + \cos \theta \hat{\mathbf{e}}_2 \end{aligned} \tag{41}$$

substitution of (41) into (40) leads, after some straightforward computations, to the following closed form solution for  $\theta$ :

$$\theta = \text{atan} \left[ \frac{\bar{\varepsilon}_{12}^0 \pm \sqrt{(\bar{\varepsilon}_{12}^0)^2 - \bar{\varepsilon}_{11}^0 \bar{\varepsilon}_{22}^0}}{\bar{\varepsilon}_{11}^0} \right]_{\mathcal{S}} \tag{42}$$

providing two different possible solutions for the normal. Additional considerations for 2-D cases are given in Appendix III.

An alternative, and completely equivalent, way to compute  $\mathbf{n}$  emerges from (37). Multiplying both sides of (37) by  $\bar{\boldsymbol{\varepsilon}}_{\mathcal{S}}^0$  and taking into account (36) we get

$$\bar{\boldsymbol{\varepsilon}}_{\mathcal{S}}^0 : \mathbf{C} \cdot \mathbf{n} \cdot [\dot{\mathbf{u}}]_{\mathcal{S}}^0 = \boldsymbol{\sigma}_{\mathcal{S}}^0 \cdot \mathbf{n} \cdot [\dot{\mathbf{u}}]_{\mathcal{S}}^0 = \frac{\dot{g}_{\mathcal{S}}^0}{\mathcal{H}} \boldsymbol{\sigma}_{\mathcal{S}}^0 : \mathbf{C}^{-1} : \boldsymbol{\sigma}_{\mathcal{S}}^0 \tag{43}$$

and thus

$$\frac{\dot{g}_{\mathcal{S}}^0}{\mathcal{H}} = \frac{\boldsymbol{\sigma}_{\mathcal{S}}^0 \cdot \mathbf{n} \cdot [\dot{\mathbf{u}}]_{\mathcal{S}}^0}{\boldsymbol{\sigma}_{\mathcal{S}}^0 : \mathbf{C}^{-1} : \boldsymbol{\sigma}_{\mathcal{S}}^0} \tag{44}$$

Now, premultiplying both sides of (37) times  $\mathbf{n}$  one gets

$$\mathbf{n} \cdot \mathbf{C} \cdot \mathbf{n} \cdot [\dot{\mathbf{u}}]_{\mathcal{S}}^0 = \frac{\dot{g}_{\mathcal{S}}^0}{\mathcal{H}} \mathbf{n} \cdot \boldsymbol{\sigma}_{\mathcal{S}}^0 \tag{45}$$

and substituting (44) into (45) we arrive at

$$\mathbf{n} \cdot \mathbf{C} \cdot \mathbf{n} \cdot [\dot{\mathbf{u}}]_{\mathcal{S}}^0 - \frac{\mathbf{n} \cdot \boldsymbol{\sigma}_{\mathcal{S}}^0 \otimes \boldsymbol{\sigma}_{\mathcal{S}}^0 \cdot \mathbf{n}}{\boldsymbol{\sigma}_{\mathcal{S}}^0 : \mathbf{C}^{-1} : \boldsymbol{\sigma}_{\mathcal{S}}^0} \cdot [\dot{\mathbf{u}}]_{\mathcal{S}}^0 = 0 \tag{46}$$

Equation (46) can be rearranged as follows (see (13)):

$$\mathbf{Q}_\nu^{d^0}(\mathbf{n}) \cdot \llbracket \dot{\mathbf{u}} \rrbracket_\nu^0 = 0 \tag{47}$$

$$\mathbf{Q}_\nu^{d^0}(\mathbf{n}) = \mathbf{n} \cdot \mathcal{E}_\nu^{d^0} \cdot \mathbf{n} \tag{48}$$

$$\mathcal{E}_\nu^{d^0} = \mathbf{C} - \frac{\boldsymbol{\sigma}_\nu^0 \otimes \boldsymbol{\sigma}_\nu^0}{\boldsymbol{\sigma}_\nu^0 : \mathbf{C}^{-1} : \boldsymbol{\sigma}_\nu^0} = \mathbf{C} - \frac{\boldsymbol{\sigma}_\nu^0 \otimes \boldsymbol{\sigma}_\nu^0}{(\tau_\nu^\sigma)^2} \tag{49}$$

Inspection of (49) in comparison to (15) states that  $\mathcal{E}_\nu^{d^0}$  is the elasto-damage tangent constitutive tensor at the initiation time (when  $d = 0$  and  $\tau_0 = \tau^\sigma$ ) for a null value of the hardening-softening parameter  $\mathcal{H} = 0$  (or  $\overline{\mathcal{H}} = 0$ ). Thus,  $\mathbf{Q}_\nu^{d^0}$  in (48) is the elasto-damage acoustic tensor at the initiation time for null softening. The existence of solutions  $\llbracket \dot{\mathbf{u}} \rrbracket_\nu^0 \neq \mathbf{0}$  for (47) implies the singularity of the acoustic tensor, that is

$$\det[\mathbf{Q}_\nu^{d^0}(\mathbf{n})] = 0 \tag{50}$$

which can be solved for  $\mathbf{n}$ .

*Remark 8.* Observe the similarity of the previous procedure for the determination of  $\mathbf{n}$  with the ones used in failure analysis based on the acoustic tensor.<sup>19</sup> It is emphasized, however, that in the present strong discontinuity analysis the considered acoustic tensor corresponds to the initiation time and to a zero value of the softening parameter.

#### 4.5. Dissipation: The fracture energy

From the principle of the expended power, and neglecting the kinetic energy, the external energy supplied to the body along the time interval  $[t_1, t_2]$  can be expressed as

$$\begin{aligned} W_{\text{ext}} \Big|_1^2 &= \int_{t_1}^{t_2} \left[ \int_{\Omega} \boldsymbol{\sigma} : \dot{\boldsymbol{\varepsilon}} \, d\Omega \right] dt = \int_{t_1}^{t_2} \left[ \int_{\Omega} (\dot{\Psi} + \mathcal{D}) \, d\Omega \right] dt \\ &= \int_{\Omega} \left[ (\Psi_2 - \Psi_1) + \int_{t_1}^{t_2} \mathcal{D} \, dt \right] d\Omega \end{aligned} \tag{51}$$

where  $\Psi$  and  $\mathcal{D}$  stand for the Helmholtz free energy and the dissipation, respectively, which from (5), (6) and (16)–(18) can be written as

$$\Psi = \frac{1}{2} \boldsymbol{\sigma} : \boldsymbol{\varepsilon} \tag{52}$$

$$\mathcal{D} = \frac{1}{2\mathcal{H}} (\tau^\sigma)^2 \dot{g} = \frac{r_0}{2\mathcal{H}} \dot{\tau}^\sigma = \delta_\nu \frac{r_0}{2\overline{\mathcal{H}}} \dot{\tau}_\nu^\sigma \tag{53}$$

Let us imagine the deformation process leading to the formation of the strong discontinuity along  $\mathcal{S}$  as follows: the process starts at time  $t_0 = 0$  with  $(\Psi_0, \tau_0^\sigma, d_0) = (0, 0, 0)$ , then the stresses increase elastically (with no dissipation) until the initial threshold value  $r_0$  is reached at time  $t_1$  when  $(\Psi_1, \tau_1^\sigma, d_1) = (\frac{1}{2}r_0^2, r_0, 0)$ . Finally a monotonic loading process ( $\dot{d} \neq 0$ ) is driven up to the total stress relaxation at time  $t_2$  with  $(\Psi_2, \tau_2^\sigma, d_2) = (0, 0, 1)$ . According to (51) and (53) the external

energy supplied along the process can be computed as

$$\begin{aligned}
 W_{\text{ext}} \Big|_0^2 &= \int_{\Omega} \left[ \underbrace{(\Psi_2)}_{=0} - \underbrace{(\Psi_0)}_{=0} + \int_{t_1}^{t_2} \mathcal{D} \, dt \right] d\Omega = \int_{t_1}^{t_2} \left[ \int_{\Omega} \delta_{\mathcal{S}} \frac{r_0}{2\mathcal{H}} \dot{\tau}_{\mathcal{S}}^{\sigma} \, d\Omega \right] dt \\
 &= \int_{t_1}^{t_2} \left[ \int_{\mathcal{S}} \frac{r_0}{2\mathcal{H}} \dot{\tau}_{\mathcal{S}}^{\sigma} d\Gamma \right] dt = \int_{\mathcal{S}} \frac{r_0}{2\mathcal{H}} \left[ \int_{\tau_1^{\sigma}}^{\tau_2^{\sigma}} d\tau^{\sigma} \right] d\Gamma \\
 &= \int_{\mathcal{S}} \frac{r_0}{2\mathcal{H}} \left[ \underbrace{\tau_2^{\sigma}}_{=0} - \underbrace{\tau_1^{\sigma}}_{=r_0} \right] d\Gamma = \int_{\mathcal{S}} -\frac{r_0^2}{2\mathcal{H}} d\Gamma
 \end{aligned} \tag{54}$$

Thus, the kernel of the last integral in (54) corresponds to the supplied energy per unit surface of the discontinuity path  $\mathcal{S}$ , which can be immediately identified as the so called *fracture energy*  $G_f$ , that is

$$G_f = -\frac{r_0^2}{2\mathcal{H}} \tag{55}$$

and considering (12)<sub>1</sub>; equation (55) can be solved for  $\overline{\mathcal{H}}$ :

$$\overline{\mathcal{H}} = -\frac{r_0^2}{2G_f} = -\frac{\sigma_u^2}{2G_f E} \tag{56}$$

which states that *the intrinsic softening parameter  $\overline{\mathcal{H}}$  is a material property related to the fracture energy  $G_f$ , Young's modulus  $E$  and uniaxial peak stress  $\sigma_u$  through (56). The negative value of  $\overline{\mathcal{H}}$  is also stated there.*

## 5. STRONG DISCONTINUITY ANALYSIS FOR PLASTICITY MODELS

### 5.1. A plasticity model with strain softening

We now consider the family of elastoplasticity models. For the sake of simplicity, we will restrict to the classical associative rate-independent model defined by

$$\dot{\boldsymbol{\sigma}} = \mathbf{C} : (\dot{\boldsymbol{\varepsilon}} - \dot{\boldsymbol{\varepsilon}}^p) \tag{57}$$

$$\dot{\boldsymbol{\varepsilon}}^p = \lambda \frac{\partial \phi}{\partial \boldsymbol{\sigma}} \tag{58}$$

$$\dot{q} = -\lambda \mathcal{H} \frac{\partial \phi}{\partial q} \tag{59}$$

$$\phi(\boldsymbol{\sigma}, q) = \hat{\phi}(\boldsymbol{\sigma}) + q - \sigma_y \tag{60}$$

$$\lambda \geq 0, \quad \phi(\boldsymbol{\sigma}, q) \leq 0, \quad \lambda \phi(\boldsymbol{\sigma}, q) = 0 \tag{61}$$

where  $\boldsymbol{\sigma}$ ,  $\boldsymbol{\varepsilon}$  and  $\boldsymbol{\varepsilon}^p$  are the stress, strain and plastic strain tensors, respectively,  $\mathbf{C}$  is the isotropic elastic constitutive tensor,  $q$  is the stress-like internal variable,  $\hat{\phi}(\boldsymbol{\sigma})$  is an homogeneous (degree one) function,  $\sigma_y > 0$  is the flow stress and  $\mathcal{H}$  is the softening parameter assumed to be negative ( $\mathcal{H} < 0$ ). Equations (61) are the classical Kuhn–Tucker conditions allowing for the determination of the plastic multiplier  $\lambda$  which can be computed from the consistency condition  $\dot{\phi} = 0$ , in terms

of  $\dot{\boldsymbol{\sigma}}$  or  $\dot{\boldsymbol{\varepsilon}}$ , as

$$\lambda = \frac{1}{\mathcal{H}} \frac{\partial \hat{\phi}}{\partial \boldsymbol{\sigma}} : \dot{\boldsymbol{\sigma}} = \frac{1}{\mathcal{H}} \nabla \hat{\phi} : \dot{\boldsymbol{\sigma}} = -\frac{1}{\mathcal{H}} \dot{q} \quad (62)$$

$$\lambda = \frac{\nabla \hat{\phi} : \mathbf{C}}{\mathcal{H} + \nabla \hat{\phi} : \mathbf{C} : \nabla \hat{\phi}} : \dot{\boldsymbol{\varepsilon}} \quad (63)$$

Substitution of (62) and (63) into (57) leads to the classical elastoplastic tangent constitutive tensor  $\mathcal{C}^{\text{ep}}$  defined by

$$\dot{\boldsymbol{\sigma}} = \mathcal{C}^{\text{ep}} : \dot{\boldsymbol{\varepsilon}} \quad (64)$$

$$\mathcal{C}^{\text{ep}} = \mathbf{C} - \frac{\mathbf{C} : \nabla \hat{\phi} \otimes \nabla \hat{\phi} : \mathbf{C}}{\mathcal{H} + \nabla \hat{\phi} : \mathbf{C} : \nabla \hat{\phi}} \quad (65)$$

and, conversely, the elastoplastic compliance constitutive tensor  $\mathcal{C}^{\text{ep}-1}$  can be defined as

$$\dot{\boldsymbol{\varepsilon}} = \mathcal{C}^{\text{ep}-1} : \dot{\boldsymbol{\sigma}} \quad (66)$$

$$\mathcal{C}^{\text{ep}-1} = \mathbf{C}^{-1} + \frac{1}{\mathcal{H}} \nabla \hat{\phi} \otimes \nabla \hat{\phi} \quad (67)$$

Finally, the dissipation  $\mathcal{D}$  can be computed as

$$\mathcal{D} = \sigma_y \lambda = -\frac{1}{\mathcal{H}} \sigma_y \dot{q} \geq 0 \quad (68)$$

## 5.2. Condition (I): Stress boundedness

Taking time derivatives of (3) and considering the material surface character of the discontinuity surface  $\mathcal{S}$  ( $\dot{\mathbf{n}} = 0$ ) we arrive at

$$\dot{\boldsymbol{\varepsilon}} = \dot{\bar{\boldsymbol{\varepsilon}}} + \delta_{\mathcal{S}} ([[\dot{\mathbf{u}}]] \otimes \mathbf{n})^{\text{S}} \quad (69)$$

and substituting (69) into (66) and then into (67),

$$\underbrace{\dot{\bar{\boldsymbol{\varepsilon}}}}_{\text{bounded}} + \underbrace{\delta_{\mathcal{S}} ([[\dot{\mathbf{u}}]]_{\nu} \otimes \mathbf{n})^{\text{S}}}_{\text{unbounded}} = \underbrace{\mathbf{C}^{-1} : \dot{\boldsymbol{\sigma}}}_{\text{bounded}} + \frac{1}{\mathcal{H}} \underbrace{\nabla \hat{\phi} \otimes \nabla \hat{\phi} : \dot{\boldsymbol{\sigma}}}_{\text{bounded}} \quad (70)$$

If we require the stress field  $\boldsymbol{\sigma}$  (and also  $\dot{\boldsymbol{\sigma}}$ ) to be bounded, the unbounded term on the left-hand side of (70) needs to be cancelled in order that  $[[\dot{\mathbf{u}}]]_{\nu}$  be non-zero. In view of (70) this cancellation can only be achieved if a delta function appears in the structure of  $1/\mathcal{H}$  so that

$$\frac{1}{\mathcal{H}} = \delta_{\mathcal{S}} \frac{1}{\mathcal{H}} + \frac{1}{\mathcal{H}^*} \quad (71)$$

As in Section 4.2 we will consider the simplest case ( $1/\mathcal{H}^* = 0$ ) so that

$$\frac{1}{\mathcal{H}} = \delta_{\mathcal{S}} \frac{1}{\mathcal{H}} \quad (72)$$

from which the distributional character of the softening parameter  $\mathcal{H}$  emerges in terms of the intrinsic softening parameter  $\mathcal{H}$ .

Now, substituting (72) into (70) and cancelling the bounded terms in the continuous domain  $\Omega \setminus \mathcal{S}$  and the unbounded terms in the discontinuity surface  $\mathcal{S}$  we arrive at

$$\dot{\bar{\mathbf{e}}} = \mathbf{C}^{-1} : \dot{\boldsymbol{\sigma}}_{\Omega \setminus \mathcal{S}} \implies \dot{\boldsymbol{\sigma}}_{\Omega \setminus \mathcal{S}} = \mathbf{C} : \dot{\bar{\mathbf{e}}} \quad (73)$$

$$([\![\dot{\mathbf{u}}]\!]_{\mathcal{S}} \otimes \mathbf{n})^S = \frac{1}{\mathcal{H}} \nabla \hat{\phi}_{\mathcal{S}} \otimes \nabla \hat{\phi}_{\mathcal{S}} : \dot{\boldsymbol{\sigma}}_{\mathcal{S}} \quad (74)$$

Equation (73) states the elastic stress–strain behaviour at the continuous part ( $\Omega \setminus \mathcal{S}$ ) of the body. Equation (74) provides a discrete constitutive equation at the discontinuity surface  $\mathcal{S}$  consistent with the original elasto plastic constitutive equation given by (57)–(61). It relates the displacement jump rate  $[\![\dot{\mathbf{u}}]\!]_{\mathcal{S}}$ , the stresses  $\boldsymbol{\sigma}_{\mathcal{S}}$  and the stress rates  $\dot{\boldsymbol{\sigma}}_{\mathcal{S}}$  at the discontinuity interface  $\mathcal{S}$ .

*Remark 9.* The same comments than in Remark (5) are applicable here. So, if (a) equation (72) (distributional character of the hardening parameter) and consequently (73) (elastic stress–strain behaviour in  $\Omega \setminus \mathcal{S}$ ) are enforced, and (b) the stresses are bounded in  $\mathcal{S}$  (by imposing a negative value of  $\bar{\mathcal{H}}$ ) (strain softening), then (74) need not to be explicitly imposed and they are implicitly fulfilled from the elastoplastic constitutive equation (66) and (70).

*Remark 10.* Equation (74) provides the resolved rate of the jump  $[\![\dot{\mathbf{u}}]\!]_{\mathcal{S}}$  in terms of  $\dot{\boldsymbol{\sigma}}_{\mathcal{S}}$  (see Appendix II for details). For the particular case of the  $J_2$  flow theory and 2-D cases, the results can be very simplified leading to

$$\begin{aligned} [\![\dot{\mathbf{u}}]\!]_{n_{\mathcal{S}}} &= 0 \\ [\![\dot{\mathbf{u}}]\!]_{p_{\mathcal{S}}} &= \dot{\gamma}_{\mathcal{S}} = \frac{3}{\mathcal{H}} \dot{\tau}_{\mathcal{S}} \end{aligned} \quad (75)$$

where  $[\![\mathbf{u}]\!]_{n_{\mathcal{S}}}$  and  $[\![\mathbf{u}]\!]_{p_{\mathcal{S}}} = \gamma_{\mathcal{S}}$  are the normal and the tangential components of the displacement jump, respectively, and  $\tau_{\mathcal{S}}$  is the shear stress along the discontinuity line  $\mathcal{S}$ . Therefore, (75) state that using the  $J_2$  flow theory only slip lines ( $[\![\dot{\mathbf{u}}]\!]_n = 0$ ), ruled by the simple discrete stress–displacement (75)<sub>2</sub>, can be modelled.

### 5.3. Condition (II): Traction vector continuity

Traction vector continuity across  $\mathcal{S}$  reads

$$\boldsymbol{\sigma}_{\Omega \setminus \mathcal{S}} \big|_{\mathbf{x} \in \mathcal{S}} \cdot \mathbf{n} = \boldsymbol{\sigma}_{\mathcal{S}} \cdot \mathbf{n} \quad (76)$$

or, taking time derivatives in (76) (and considering  $\dot{\mathbf{n}} = 0$ ),

$$\dot{\boldsymbol{\sigma}}_{\Omega \setminus \mathcal{S}} \big|_{\mathbf{x} \in \mathcal{S}} \cdot \mathbf{n} = \dot{\boldsymbol{\sigma}}_{\mathcal{S}} \cdot \mathbf{n} \quad (77)$$

Unlike in damage models, equation (74) cannot be explicitly inverted, to solve for  $\dot{\boldsymbol{\sigma}}_{\mathcal{S}}$ , due to the incomplete range of the fourth-order tensor  $\nabla \hat{\phi}_{\mathcal{S}} \otimes \nabla \hat{\phi}_{\mathcal{S}}$ . The full determination of the stress field has to be done in conjunction with the equations provided by the traction vector continuity requirement so that, finally, (74) and (76) or (77) provide a well-posed, in general non-linear, system of equations allowing for the determination of the jump  $[\![\mathbf{u}]\!]_{\mathcal{S}}$  and the stress field  $\boldsymbol{\sigma}_{\mathcal{S}}$  at the discontinuity surface.

#### 5.4. Condition (III): Identification of the normal

Equations (74) can be written at the initiation time  $t_0$  as

$$\begin{aligned} ([\dot{\mathbf{u}}]_{\mathcal{S}}^0 \otimes \mathbf{n})^S &= \gamma^0 \nabla \hat{\phi}(\boldsymbol{\sigma}_{\mathcal{S}}^0) \\ \gamma^0 &= \frac{\nabla \hat{\phi}_{\mathcal{S}}^0 : \dot{\boldsymbol{\sigma}}_{\mathcal{S}}^0}{\mathcal{H}} = \frac{\dot{\hat{\phi}}_{\mathcal{S}}^0}{\mathcal{H}} \end{aligned} \quad (78)$$

Equation (78) provides a set of equations similar to the ones obtained for the damage model (see (38)) but now in terms of the stresses  $\boldsymbol{\sigma}_{\mathcal{S}}^0$  instead of the strains  $\bar{\boldsymbol{\epsilon}}_{\mathcal{S}}^0$ . Thus, a similar procedure to the one explained in Section 4.4 can be applied here for the obtention of  $\mathbf{n}$  leading to

$$\mathbf{t} \cdot \nabla \hat{\phi}_{\mathcal{S}}^0 \cdot \mathbf{t} = 0 \quad \forall \mathbf{t} | \mathbf{t} \cdot \mathbf{n} = 0 \quad (79)$$

As said in Remark (7), for 2-D cases the inclination angle  $\theta$  of the normal with respect to an orthogonal basis  $\hat{\mathbf{e}}_1, \hat{\mathbf{e}}_2$  can be explicitly computed in terms of the components of  $\nabla \hat{\phi}_{\mathcal{S}}^0$  as

$$\theta = \text{atan} \left[ \frac{\nabla \hat{\phi}_{12}^0 \pm \sqrt{(\nabla \hat{\phi}_{12}^0)^2 - \nabla \hat{\phi}_{11}^0 \nabla \hat{\phi}_{22}^0}}{\nabla \hat{\phi}_{11}^0} \right]_{\mathcal{S}} \quad (80)$$

For the particular case of J2 flow theory and 2-D (plane-strain, plane-stress) cases, closed-form expressions of  $\theta$ , in terms of the deviatoric stress field either at  $\mathcal{S}$  or at  $\Omega \setminus \mathcal{S}$  can be derived (see Appendix III).

An alternative procedure for the computation of  $\mathbf{n}$  can be obtained following the same steps as in Section 4.4. For the damage model: multiplying both sides of (78)<sub>1</sub> times  $\nabla \hat{\phi}_{\mathcal{S}}^0 : \mathbf{C}$  we get

$$\nabla \hat{\phi}_{\mathcal{S}}^0 : \mathbf{C} : ([\dot{\mathbf{u}}]_{\mathcal{S}}^0 \otimes \mathbf{n})^S = \gamma^0 \nabla \hat{\phi}^0 : \mathbf{C} : \nabla \hat{\phi}_{\mathcal{S}}^0$$

thus,

$$\gamma^0 = \frac{\nabla \hat{\phi}_{\mathcal{S}}^0 : \mathbf{C} : [\dot{\mathbf{u}}]_{\mathcal{S}}^0 \cdot \mathbf{n}}{\nabla \hat{\phi}_{\mathcal{S}}^0 : \mathbf{C} : \nabla \hat{\phi}_{\mathcal{S}}^0} \quad (81)$$

Now, multiplying (78)<sub>1</sub> times  $\mathbf{n} \cdot \mathbf{C}$  we obtain

$$\mathbf{n} \cdot \mathbf{C} : ([\dot{\mathbf{u}}]_{\mathcal{S}}^0 \otimes \mathbf{n}) = \mathbf{n} \cdot \mathbf{C} \cdot \mathbf{n} \cdot [\dot{\mathbf{u}}]_{\mathcal{S}}^0 = \mathbf{n} \cdot \mathbf{C} : \nabla \hat{\phi}_{\mathcal{S}}^0 \gamma^0 \quad (82)$$

and substituting (81) into (82) we arrive at

$$\mathbf{n} \cdot \mathbf{C} \cdot \mathbf{n} \cdot [\dot{\mathbf{u}}]_{\mathcal{S}}^0 - \mathbf{n} \cdot \frac{\mathbf{C} : \nabla \hat{\phi}_{\mathcal{S}}^0 \otimes \nabla \hat{\phi}_{\mathcal{S}}^0 : \mathbf{C}}{\nabla \hat{\phi}_{\mathcal{S}}^0 : \mathbf{C} : \nabla \hat{\phi}_{\mathcal{S}}^0} \cdot \mathbf{n} \cdot [\dot{\mathbf{u}}]_{\mathcal{S}}^0 = 0 \quad (83)$$

Equation (83) can be rearranged as follows:

$$\mathbf{Q}_{\mathcal{S}}^{\text{ep}0}(\mathbf{n}) \cdot [\dot{\mathbf{u}}]_{\mathcal{S}}^0 = 0 \quad (84)$$

$$\mathbf{Q}_{\mathcal{S}}^{\text{ep}0}(\mathbf{n}) = \mathbf{n} \cdot \mathcal{E}_{\mathcal{S}}^{\text{ep}0} \cdot \mathbf{n} \quad (85)$$

$$\mathcal{E}_{\mathcal{S}}^{\text{ep}0} = \mathbf{C} - \frac{\mathbf{C} : \nabla \hat{\phi}_{\mathcal{S}}^0 \otimes \nabla \hat{\phi}_{\mathcal{S}}^0 : \mathbf{C}}{\nabla \hat{\phi}_{\mathcal{S}}^0 : \mathbf{C} : \nabla \hat{\phi}_{\mathcal{S}}^0} \quad (86)$$

The existence of solutions  $[\dot{\mathbf{u}}]_{\mathcal{S}}^0 \neq 0$  in (84) implies the singularity of the elastoplastic acoustic tensor  $\mathbf{Q}_{\mathcal{S}}^{\text{ep}0}(\mathbf{n})$ , so that

$$\det[\mathbf{Q}_{\mathcal{S}}^{\text{ep}0}(\mathbf{n})] = 0 \tag{87}$$

from which  $\mathbf{n}$  can be computed. Observe in (85) and (86) that  $\mathbf{Q}_{\mathcal{S}}^{\text{ep}0}$  is given in terms of  $\mathcal{C}_{\mathcal{S}}^{\text{ep}0}$  which is the elastoplastic tangent constitutive tensor at the initiation time *with null hardening* as can be checked by comparison with (65).

5.5. Dissipation: The fracture energy

From (68) and taking into account (72) the dissipation can be written as

$$\mathcal{D} = -\frac{1}{\mathcal{H}} \sigma_y \dot{q} = -\delta_{\mathcal{S}} \frac{1}{\mathcal{H}} \sigma_y \dot{q} \tag{88}$$

where, during plastic loading,  $q$  can be computed from the consistency equation  $\phi(\boldsymbol{\sigma}, q) = 0$  and, consequently, from (60):

$$q = \sigma_y - \hat{\phi}(\boldsymbol{\sigma}) \tag{89}$$

Notice that  $\hat{\phi}(\mathbf{0}) = 0$  due to the homogeneous character of the function  $\hat{\phi}(\cdot)$ . On the other hand, the free energy can be expressed, considering (72), as

$$\Psi = \frac{1}{2} \boldsymbol{\sigma} : \mathbf{C}^{-1} : \boldsymbol{\sigma} + \frac{1}{2} \frac{q^2}{\mathcal{H}} = \frac{1}{2} \boldsymbol{\sigma} : \mathbf{C}^{-1} : \boldsymbol{\sigma} + \frac{1}{2} \delta_{\mathcal{S}} \frac{q^2}{\mathcal{H}} \tag{90}$$

Like in Section 4.5, let us consider the deformation process leading to the formation of the strong discontinuity as follows: the process starts at time  $t_0 = 0$ , with  $(\Psi_0, q_0) = (0, 0)$ . Then the strains are elastically increased (with no dissipation) up to the initiation of the plastic flow at time  $t_1$  (the initiation time). Beyond this point the strain-softening constitutive equation leads to the full relaxation of the stresses at time  $t_2$  where  $\hat{\phi}(\boldsymbol{\sigma}_2) = \hat{\phi}(\mathbf{0}) = 0$  and thus  $q_2 = \sigma_y$  from (89). Consequently,  $(\Psi_2, q_2) = (\frac{1}{2} \delta_{\mathcal{S}} (\sigma_y^2 / \mathcal{H}), \sigma_y)$ . The externally supplied energy can be then expressed from (51) as

$$\begin{aligned} W_{\text{ext}} \Big|_0^2 &= \int_{\Omega} \left[ (\Psi_2 - \Psi_0) + \int_{t_1}^{t_2} \mathcal{D} dt \right] d\Omega \\ &= \int_{\Omega} \delta_{\mathcal{S}} \left[ \frac{1}{2} \frac{\sigma_y^2}{\mathcal{H}} - \int_{t_1}^{t_2} \frac{\sigma_y}{\mathcal{H}} \dot{q} dt \right] d\Omega = \int_{\mathcal{S}} \left[ \frac{1}{2} \frac{\sigma_y^2}{\mathcal{H}} - \int_{t_1}^{t_2} \frac{\sigma_y}{\mathcal{H}} \dot{q} dt \right] d\Gamma \\ &= \int_{\mathcal{S}} \left[ \frac{1}{2} \frac{\sigma_y^2}{\mathcal{H}} - \frac{\sigma_y}{\mathcal{H}} \int_{q_1=0}^{q_2=\sigma_y} dq \right] d\Gamma = \int_{\mathcal{S}} -\frac{1}{2} \frac{\sigma_y^2}{\mathcal{H}} d\Gamma \end{aligned} \tag{91}$$

Then the supplied energy per unit of discontinuity surface (*the fracture energy*) can be identified from (91) as the kernel of the last integral, i.e.

$$G_f = -\frac{1}{2} \frac{\sigma_y^2}{\mathcal{H}} \tag{92}$$

Notice again the similarity of (55) (damage model) with (92) (plasticity model). From (92) the intrinsic softening parameter  $\mathcal{H}$  can be regarded as a material property related to the fracture



energy  $G_f$  and the flow stress  $\sigma_y$  by:

$$\bar{\mathcal{H}} = -\frac{1}{2} \frac{\sigma_y^2}{G_f} \quad (93)$$

## 6. CONCLUDING REMARKS

Along the preceding sections, the methodology of applying the strong discontinuity analysis to standard (local, stress–strain) constitutive equations has been presented. The analysis defines a common framework, in which different families of constitutive equations can be considered. By imposing several requirements on the stress field, in order to make the constitutive equation *compatible* with the appearance of strong discontinuities, the analysis provides a set of equations which allows to solve for the additional unknowns appearing in the problem: the displacement jump, the stress field at the discontinuity path and the normal. As main ingredients of the resulting framework, the following should be mentioned:

- (1) The *distributional character of the softening parameter*. On one side, strain softening has to be considered for the constitutive equation at the discontinuity path. The inverse of the softening parameter must have the structure of a delta function according to (22) and (72) so that, roughly speaking, a perfect-damage or perfect-plasticity behaviour has to be approached from a *softening branch* in the constitutive equation. The intensity of the softening parameter function can be defined in terms of an *intrinsic softening parameter*  $\bar{\mathcal{H}}$  which can be proved to be a material property related to the fracture energy as shown in (56) and (93). On the other hand, an elastic (or, in the most general context, inelastic with strain-hardening) behaviour has to be considered for the constitutive equation at the continuous part of the body. Under these conditions a consistent *discrete* constitutive equation emerges which relates the stress field at the discontinuity path with the jump. However, this discrete constitutive equation has not necessarily to be explicitly computed for the different constitutive models.
- (2) The *traction vector continuity* condition provides the necessary set of additional equations to determine the jump and the stress field at the discontinuity path. Although explicit expressions for both fields can be sometimes derived, and then the analysis can be continued in a *discrete* environment (see, for instance, Reference [17]), the crucial fact is the necessity of imposition of such condition in the context of strong discontinuity problems.
- (3) The normal to the discontinuity path can be determined by imposition of the material surface character of the discontinuity surface at the initiation time), this leading to simple expressions, in terms of the regular strain (damage models) or the stress (plasticity models) fields, which, however, have to be specifically determined for each family of constitutive equations.

This general framework plays a crucial role in the design of appropriate numerical approaches to the strong discontinuity problems. This subject will be addressed in Part II of this work.

## APPENDIX I

### I.1 Some alternatives for the continuum damage model

Non-symmetric tension-compression behaviour. The strain norm  $\tau^e$  in (11) can be rewritten in terms of the so-called *effective stress*  $\bar{\sigma} = \mathbf{C} : \boldsymbol{\varepsilon}$  as

$$\tau^e = \sqrt{\bar{\sigma} : \boldsymbol{\varepsilon}} \quad (94)$$

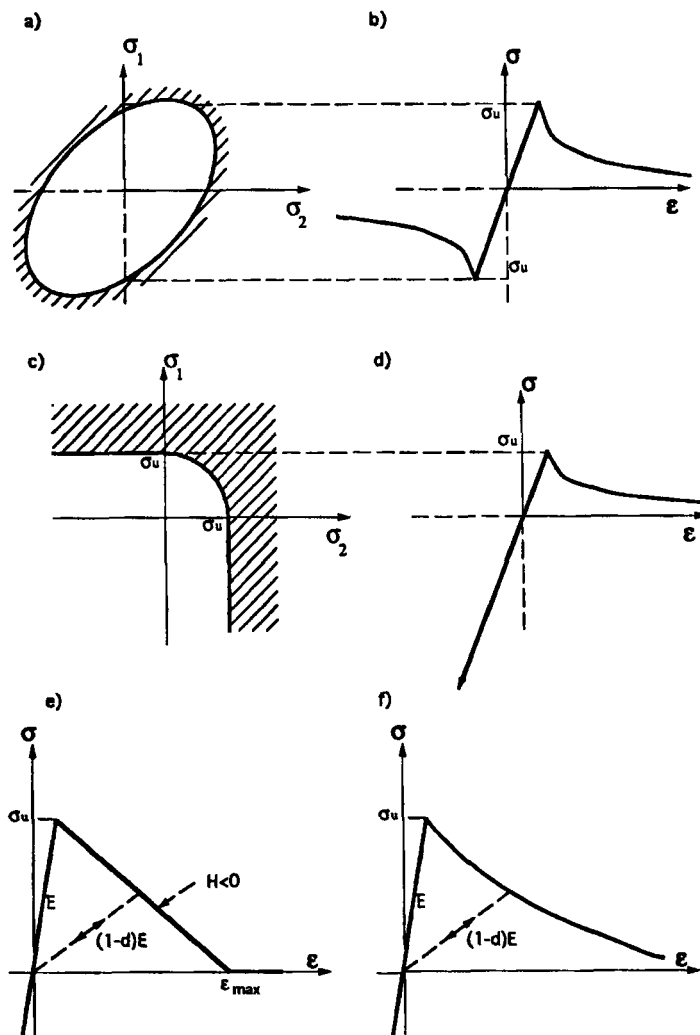


Figure 4. Different alternatives for the continuum damage model

The corresponding damage model is symmetric in the tension-compression domains as can be checked in Figures 4(a) and 4(b). A more realistic approach for many geomaterials, in which the maximum compressive strength is much higher than the maximum tensile strength, can be obtained by modifying (94) as follows:<sup>7</sup>

$$\hat{\tau}^e = \sqrt{\sum_1^3 \langle \bar{\sigma}_i \rangle \varepsilon_i} \quad (95)$$

where  $\bar{\sigma}_i$  and  $\varepsilon_i$  are the principal stress and strain components, respectively, and  $\langle \cdot \rangle$  is the Mc.Auley bracket. Due to the isotropic character of the elastic tensor  $C$ , the principal directions of both tensors coincide. The corresponding initial elastic domain, in the principal stress space, and the uniaxial stress-strain law are depicted in Figures 4(c) and 4(d), respectively. Observe that this domain is open in the pure compression octant which guarantees a linear elastic behaviour in this domain.

Exponential softening. Equation (12)<sub>2</sub> defines a linear strain-softening law (see Figure 4(e)). An alternative exponential softening law can be defined as:<sup>7</sup>

$$d = G(r) = 1 - \frac{r_0}{r} e^{\mathcal{H}(r/r_0 - 1)} \tag{96}$$

where  $\mathcal{H}$  plays the role of softening parameter ( $\mathcal{H} < 0$ ). The corresponding uniaxial stress-strain law is depicted in Figure 4(f).

APPENDIX II

II. 1. Resolved jumps

Let us consider the equation

$$([\mathbf{u}] \otimes \mathbf{n})^S = \mathbf{A}, \quad \mathbf{A}^T = \mathbf{A} \tag{97}$$

and the orthogonal basis constituted by  $\mathbf{n}$  and any two (mutually orthogonal) unit vectors  $\mathbf{p}$  and  $\mathbf{q}$  such that

$$\mathbf{n} \cdot \mathbf{p} = \mathbf{n} \cdot \mathbf{q} = \mathbf{p} \cdot \mathbf{q} = 0, \quad |\mathbf{n}| = |\mathbf{p}| = |\mathbf{q}| = 1 \tag{98}$$

Let

$$\begin{bmatrix} A_{nn} & A_{np} & A_{nq} \\ A_{np} & A_{pp} & A_{pq} \\ A_{nq} & A_{pq} & A_{qq} \end{bmatrix} \tag{99}$$

be the matrix of components of  $\mathbf{A}$  in the chosen basis. It is straightforward to check that the following relations hold:

$$\begin{aligned} A_{pp} &= \mathbf{p} \cdot \mathbf{A} \cdot \mathbf{p} = \mathbf{p} \cdot ([\mathbf{u}] \otimes \mathbf{n})^S \cdot \mathbf{p} = 0 \\ A_{qq} &= \mathbf{q} \cdot \mathbf{A} \cdot \mathbf{q} = \mathbf{q} \cdot ([\mathbf{u}] \otimes \mathbf{n})^S \cdot \mathbf{q} = 0 \\ A_{pq} &= \mathbf{p} \cdot \mathbf{A} \cdot \mathbf{q} = \mathbf{p} \cdot ([\mathbf{u}] \otimes \mathbf{n})^S \cdot \mathbf{q} = 0 \end{aligned} \tag{100a}$$

$$\begin{aligned} A_{nn} &= \mathbf{n} \cdot \mathbf{A} \cdot \mathbf{n} = \mathbf{n} \cdot ([\mathbf{u}] \otimes \mathbf{n})^S \cdot \mathbf{n} = [\mathbf{u}] \cdot \mathbf{n} = [\mathbf{u}]_n \\ A_{np} &= \mathbf{n} \cdot \mathbf{A} \cdot \mathbf{p} = \mathbf{n} \cdot ([\mathbf{u}] \otimes \mathbf{n})^S \cdot \mathbf{p} = \frac{1}{2} [\mathbf{u}] \cdot \mathbf{p} = \frac{1}{2} [\mathbf{u}]_p \\ A_{nq} &= \mathbf{n} \cdot \mathbf{A} \cdot \mathbf{q} = \mathbf{n} \cdot ([\mathbf{u}] \otimes \mathbf{n})^S \cdot \mathbf{q} = \frac{1}{2} [\mathbf{u}] \cdot \mathbf{q} = \frac{1}{2} [\mathbf{u}]_q \end{aligned} \tag{100b}$$

where  $[\mathbf{u}]_n$ ,  $[\mathbf{u}]_p$  and  $[\mathbf{u}]_q$  are, respectively, the components of the jump  $[\mathbf{u}]$  in  $\mathbf{n}, \mathbf{p}, \mathbf{q}$ . So, from (100) we can write

$$\begin{aligned} [\mathbf{u}]_n &= [\mathbf{u}] \cdot \mathbf{n} = A_{nn} \\ [\mathbf{u}]_p &= [\mathbf{u}] \cdot \mathbf{p} = 2A_{np} \\ [\mathbf{u}]_q &= [\mathbf{u}] \cdot \mathbf{q} = 2A_{nq} \end{aligned} \tag{101}$$

*II.1.1. Resolved jump for the isotropic damage model.* From (25), tensor  $\mathbf{A}$  in (97) can be identified as:

$$\mathbf{A} = \frac{g_{,s}}{\mathcal{H}} \mathbf{C}^{-1} : \boldsymbol{\sigma}_{,s} = \frac{g_{,s}}{\mathcal{H}} \left[ -\frac{\nu}{E} \text{tr}(\boldsymbol{\sigma}_{,s}) \mathbf{1} + \frac{1+\nu}{E} \boldsymbol{\sigma}_{,s} \right] \quad (102)$$

where  $\text{tr}(\cdot)$  means the trace,  $\mathbf{1}$  is the second-order unit tensor and the expression of  $\mathbf{C}^{-1}$  (the elastic compliance fourth-order tensor) in terms of Poisson's ratio  $\nu$  and Young's modulus  $E$  has been considered. From (100a) and (102):

$$\begin{aligned} A_{pp} &= \mathbf{p} \cdot \mathbf{A} \cdot \mathbf{p} = \frac{g_{,s}}{\mathcal{H}} \frac{1}{E} \left[ (\sigma_{pp,s} - \nu(\sigma_{nn,s} + \sigma_{qq,s})) \right] = 0 \\ A_{qq} &= \mathbf{q} \cdot \mathbf{A} \cdot \mathbf{q} = \frac{g_{,s}}{\mathcal{H}} \frac{1}{E} \left[ (\sigma_{qq,s} - \nu(\sigma_{nn,s} + \sigma_{pp,s})) \right] = 0 \\ A_{pq} &= \mathbf{p} \cdot \mathbf{A} \cdot \mathbf{q} = \frac{g_{,s}}{\mathcal{H}} \frac{(1+\nu)}{E} \sigma_{pq,s} = 0 \end{aligned} \quad (103)$$

so that (103) leads to the following values for the stresses:

$$\begin{aligned} \sigma_{pp,s} &= \frac{\nu}{1-\nu} \sigma_{nn,s} \\ \sigma_{qq,s} &= \frac{\nu}{1-\nu} \sigma_{nn,s} \\ \sigma_{pq,s} &= 0 \end{aligned} \quad (104)$$

Then, from (100b) and (104) one arrives at

$$\begin{aligned} A_{nn} &= \mathbf{n} \cdot \mathbf{A} \cdot \mathbf{n} = \frac{g_{,s}}{\mathcal{H}} \frac{1}{E} \left[ (\sigma_{nn,s} - \nu(\sigma_{pp,s} + \sigma_{qq,s})) \right] \\ &= \frac{g_{,s}}{\mathcal{H}} \frac{1}{E} \frac{(1+\nu)(1-2\nu)}{1-\nu} \sigma_{nn,s} \\ A_{np} &= \mathbf{n} \cdot \mathbf{A} \cdot \mathbf{p} = \frac{g_{,s}}{\mathcal{H}} \frac{1+\nu}{E} \sigma_{np,s} \\ A_{nq} &= \mathbf{n} \cdot \mathbf{A} \cdot \mathbf{q} = \frac{g_{,s}}{\mathcal{H}} \frac{1+\nu}{E} \sigma_{nq,s} \end{aligned} \quad (106)$$

Finally, from (106) and (101) we get

$$\begin{bmatrix} [\mathbf{u}]_n \\ [\mathbf{u}]_p \\ [\mathbf{u}]_q \end{bmatrix}_{,s} = \frac{g_{,s}}{\mathcal{H}} \frac{1}{E} \begin{bmatrix} \frac{(1+\nu)(1-2\nu)}{1-\nu} & 0 & 0 \\ 0 & 1+\nu & 0 \\ 0 & 0 & 1+\nu \end{bmatrix} \begin{bmatrix} \sigma_{nn} \\ \sigma_{np} \\ \sigma_{nq} \end{bmatrix}_{,s} \quad (107)$$

*II.1.2. Resolved jump for the plasticity model.* From (79), tensor  $\mathbf{A}$  of (97) can be identified as

$$\begin{aligned} \mathbf{A} &= \gamma \nabla \hat{\phi}_{,s} \\ \gamma &= \frac{1}{\mathcal{H}} \hat{\boldsymbol{\sigma}}_{,s} : \nabla \hat{\phi}(\boldsymbol{\sigma}_{,s}) = \frac{1}{\mathcal{H}} \hat{\phi}_{,s} \end{aligned} \quad (108)$$

and (100a), (100b) and (101) hold in terms of  $[[\dot{\mathbf{u}}]]_{\mathcal{S}}$ . Thus, substituting (108) into (100a) one obtains

$$\begin{aligned} A_{pp} = \mathbf{p} \cdot \mathbf{A} \cdot \mathbf{p} = 0 &\implies \mathbf{p} \cdot \nabla \hat{\phi}_{,\mathcal{S}} \cdot \mathbf{p} = 0 \implies \left. \frac{\partial \hat{\phi}(\boldsymbol{\sigma})}{\partial \sigma_{pp}} \right|_{\mathcal{S}} = 0 \\ A_{qq} = \mathbf{q} \cdot \mathbf{A} \cdot \mathbf{q} = 0 &\implies \mathbf{q} \cdot \nabla \hat{\phi}_{,\mathcal{S}} \cdot \mathbf{q} = 0 \implies \left. \frac{\partial \hat{\phi}(\boldsymbol{\sigma})}{\partial \sigma_{qq}} \right|_{\mathcal{S}} = 0 \\ A_{pq} = \mathbf{p} \cdot \mathbf{A} \cdot \mathbf{q} = 0 &\implies \mathbf{p} \cdot \nabla \hat{\phi}_{,\mathcal{S}} \cdot \mathbf{q} = 0 \implies \left. \frac{\partial \hat{\phi}(\boldsymbol{\sigma})}{\partial \sigma_{pq}} \right|_{\mathcal{S}} = 0 \end{aligned} \quad (109)$$

and substituting equation (108) into (100b),

$$\begin{aligned} A_{nn} = \mathbf{n} \cdot \mathbf{A} \cdot \mathbf{n} = \gamma \mathbf{n} \cdot \nabla \hat{\phi}_{,\mathcal{S}} \cdot \mathbf{n} &= \gamma \left. \frac{\partial \hat{\phi}(\boldsymbol{\sigma})}{\partial \sigma_{nn}} \right|_{\mathcal{S}} \\ A_{np} = \mathbf{n} \cdot \mathbf{A} \cdot \mathbf{p} = \gamma \mathbf{n} \cdot \nabla \hat{\phi}_{,\mathcal{S}} \cdot \mathbf{p} &= \gamma \left. \frac{\partial \hat{\phi}(\boldsymbol{\sigma})}{\partial \sigma_{np}} \right|_{\mathcal{S}} \\ A_{nq} = \mathbf{n} \cdot \mathbf{A} \cdot \mathbf{q} = \gamma \mathbf{n} \cdot \nabla \hat{\phi}_{,\mathcal{S}} \cdot \mathbf{q} &= \gamma \left. \frac{\partial \hat{\phi}(\boldsymbol{\sigma})}{\partial \sigma_{nq}} \right|_{\mathcal{S}} \end{aligned} \quad (110)$$

Then, from (110) the components of  $[[\dot{\mathbf{u}}]]_{\mathcal{S}}$  can be computed as (see also (101) and (108)<sub>2</sub>):

$$\begin{aligned} [[\dot{\mathbf{u}}]]_{n,\mathcal{S}} = [[\dot{\mathbf{u}}]]_{,\mathcal{S}} \cdot \mathbf{n} = A_{nn} &= \frac{1}{\mathcal{H}} \dot{\phi}_{,\mathcal{S}} \left. \frac{\partial \hat{\phi}(\boldsymbol{\sigma})}{\partial \sigma_{nn}} \right|_{\mathcal{S}} \\ [[\dot{\mathbf{u}}]]_{p,\mathcal{S}} = [[\dot{\mathbf{u}}]]_{,\mathcal{S}} \cdot \mathbf{p} = 2A_{np} &= \frac{2}{\mathcal{H}} \dot{\phi}_{,\mathcal{S}} \left. \frac{\partial \hat{\phi}(\boldsymbol{\sigma})}{\partial \sigma_{np}} \right|_{\mathcal{S}} \\ [[\dot{\mathbf{u}}]]_{q,\mathcal{S}} = [[\dot{\mathbf{u}}]]_{,\mathcal{S}} \cdot \mathbf{q} = 2A_{nq} &= \frac{2}{\mathcal{H}} \dot{\phi}_{,\mathcal{S}} \left. \frac{\partial \hat{\phi}(\boldsymbol{\sigma})}{\partial \sigma_{nq}} \right|_{\mathcal{S}} \end{aligned} \quad (111)$$

where, from (109),  $\dot{\phi}_{,\mathcal{S}}$  can be expressed only in terms of the components of the rate of the traction vector  $\dot{\boldsymbol{\sigma}}_{,\mathcal{S}} \cdot \mathbf{n} = (\dot{\sigma}_{nn}, \dot{\sigma}_{np}, \dot{\sigma}_{nq})_{,\mathcal{S}}^T$  as

$$\dot{\phi}_{,\mathcal{S}} = \left. \frac{\partial \hat{\phi}(\boldsymbol{\sigma})}{\partial \sigma_{nn}} \right|_{\mathcal{S}} \dot{\sigma}_{nn,\mathcal{S}} + 2 \left. \frac{\partial \hat{\phi}(\boldsymbol{\sigma})}{\partial \sigma_{np}} \right|_{\mathcal{S}} \dot{\sigma}_{np,\mathcal{S}} + 2 \left. \frac{\partial \hat{\phi}(\boldsymbol{\sigma})}{\partial \sigma_{nq}} \right|_{\mathcal{S}} \dot{\sigma}_{nq,\mathcal{S}} \quad (112)$$

Equations (111) and (112) provide the resolved (rate of the) displacement jump in terms of the (rate of the) stresses.

*II.1.3. Application to the  $J_2$  flow theory.* In the  $J_2$  flow theory case the yield function is defined by

$$\hat{\phi}(\boldsymbol{\sigma}) = \sqrt{\frac{3}{2} [\boldsymbol{\sigma} : \boldsymbol{\sigma} - \frac{1}{3} \text{tr}^2(\boldsymbol{\sigma})]} = \sqrt{\frac{3}{2}} \|\mathbf{S}\| \quad (113)$$

where  $\|\cdot\|$  stands for the norm and  $\mathbf{S}$  are the deviatoric stresses:

$$\mathbf{S} = \boldsymbol{\sigma} - \frac{1}{3} \text{tr}(\boldsymbol{\sigma}) \mathbf{1} \tag{114}$$

so that  $\text{tr}(\mathbf{S}) = 0$ . From (113) and (114) it is straightforward to check that

$$\nabla \hat{\phi}(\boldsymbol{\sigma}) = \sqrt{\frac{3}{2}} \frac{\mathbf{S}}{\|\mathbf{S}\|} \tag{115}$$

Thus, taking into account (115), for the  $J_2$  flow theory case, (109) states that:  $S_{pp} = S_{qq} = S_{pq} = 0$  and then  $\text{tr}(\mathbf{S}) = S_{nn} + S_{pp} + S_{qq} = 0 \implies S_{nn} = 0$  so that the deviatoric stress field reduces to

$$\mathbf{S}_{,\mathcal{F}} = \begin{bmatrix} 0 & \sigma_{np} & \sigma_{nq} \\ \sigma_{np} & 0 & 0 \\ \sigma_{nq} & 0 & 0 \end{bmatrix}_{,\mathcal{F}} \tag{116}$$

and, thus, from (113),

$$\begin{aligned} \hat{\phi}_{,\mathcal{F}} &= \sqrt{\frac{3}{2}} \|\mathbf{S}_{,\mathcal{F}}\| = \sqrt{\frac{3}{2}} (\sigma_{np,\mathcal{F}}^2 + \sigma_{pn,\mathcal{F}}^2 + \sigma_{nq,\mathcal{F}}^2 + \sigma_{qn,\mathcal{F}}^2)^{1/2} \\ &= \sqrt{3} (\sigma_{np,\mathcal{F}}^2 + \sigma_{nq,\mathcal{F}}^2)^{1/2} \end{aligned} \tag{117}$$

$$\hat{\phi}_{,\mathcal{F}} = \frac{\sqrt{3}}{(\sigma_{np,\mathcal{F}}^2 + \sigma_{nq,\mathcal{F}}^2)^{1/2}} (\sigma_{np,\mathcal{F}} \dot{\sigma}_{np,\mathcal{F}} + \sigma_{nq,\mathcal{F}} \dot{\sigma}_{nq,\mathcal{F}}) \tag{118}$$

Then, substitution of (118) into (111) taking into account (115) leads to

$$\llbracket \dot{\mathbf{u}} \rrbracket_{n,\mathcal{F}} = 0 \tag{119}$$

$$\begin{bmatrix} \llbracket \dot{\mathbf{u}} \rrbracket_p \\ \llbracket \dot{\mathbf{u}} \rrbracket_q \end{bmatrix}_{,\mathcal{F}} = \frac{3}{\mathcal{H}} \frac{1}{\sigma_{np,\mathcal{F}}^2 + \sigma_{nq,\mathcal{F}}^2} \begin{bmatrix} \sigma_{np}^2 & \sigma_{np}\sigma_{nq} \\ \sigma_{np}\sigma_{nq} & \sigma_{nq}^2 \end{bmatrix}_{,\mathcal{F}} \begin{bmatrix} \dot{\sigma}_{np} \\ \dot{\sigma}_{nq} \end{bmatrix}_{,\mathcal{F}} \tag{120}$$

Finally, for 2-D cases (plane stress–plane strain) where  $\mathbf{n}$  and  $\mathbf{p}$  define the plane of analysis and  $\sigma_{nq,\mathcal{F}}$  is assumed to be zero, equations (119) and (120) read

$$\llbracket \dot{\mathbf{u}} \rrbracket_{n,\mathcal{F}} = 0 \tag{121}$$

$$\underbrace{\llbracket \dot{\mathbf{u}} \rrbracket_p}_{,\mathcal{F}} = \frac{3}{\mathcal{H}} \underbrace{\dot{\sigma}_{np,\mathcal{F}}}_{,\mathcal{F}} \implies \dot{\gamma}_{,\mathcal{F}} = \frac{3}{\mathcal{H}} \dot{\tau}_{,\mathcal{F}} \tag{122}$$

On (121) rely some interesting properties of the stress field for the  $J_2$  flow theory case. In fact, taking the trace of (70), in view of (115) and (121), we arrive at

$$\underbrace{\text{Tr}(\dot{\bar{\mathbf{E}}})}_{\bar{\dot{\epsilon}}} + \delta_{,\mathcal{F}} \underbrace{\text{Tr}(\llbracket \dot{\mathbf{u}} \rrbracket_{,\mathcal{F}} \otimes \mathbf{n})^S}_{= \llbracket \dot{\mathbf{u}} \rrbracket_n = 0} = \frac{\dot{p}}{K} + \frac{1}{\mathcal{H}} \hat{\phi}_{,\mathcal{F}} \cdot \underbrace{\text{Tr}(\nabla \hat{\phi})}_{=0} \tag{123}$$

where  $\bar{\epsilon}$ ,  $p$ , and  $K$  stand for the regular part of the volumetric strain, the pressure (mean stress) and the bulk modulus, respectively. From (123) we conclude that  $\bar{\dot{\epsilon}} = \dot{p}/K$  and  $p_{,\mathcal{F}} = p_{\Omega \setminus \mathcal{F}} = K\bar{\epsilon}$ . Thus, (121) states, for the  $J_2$  case, the continuity of the pressure across  $S$  ( $\llbracket p \rrbracket = 0$ ). Consequently,

from the continuity of the traction vector ( $[[\boldsymbol{\sigma}]] \cdot \mathbf{n} = 0 \implies [[\sigma_{nn}]] = [[p]] + [[S_{nn}]] = 0$ ) we obtain

$$[[S_{nn}]] = 0 \implies S_{nn,\mathcal{S}} = S_{nn,\Omega \setminus \mathcal{S}}|_{x \in \mathcal{S}} \quad (124)$$

so that continuity of  $S_{nn}$  across  $\mathcal{S}$  can also be stated. Finally, since  $S_{nn,\mathcal{S}} = 0$  (see (116)) we conclude that

$$S_{nn,\Omega \setminus \mathcal{S}}|_{x \in \mathcal{S}} = 0 \quad (125)$$

Equation (125) can be used for the determination of the normal  $\mathbf{n}$  in terms of the stress field at  $\Omega \setminus \mathcal{S}$  (see Appendix III, Section III.1.2).

### APPENDIX III

#### III.1. Analysis of the discontinuity direction for 2-D cases

*III.1.1. Isotropic damage model.* Denoting by  $\mathbf{n}$  and  $\mathbf{t}$  the unit vectors normal and tangent, respectively, to the discontinuity line  $\mathcal{S}$ , and considering the orthogonal basis  $\hat{\mathbf{e}}_1, \hat{\mathbf{e}}_2$  ( $\hat{\mathbf{e}}_1 = \mathbf{n}$ ,  $\hat{\mathbf{e}}_2 = \mathbf{t}$ ), the equation

$$\mathbf{t} \cdot \bar{\boldsymbol{\varepsilon}} \cdot \mathbf{t} = \bar{\varepsilon}_{tt} = 0 \quad (126)$$

states that the regular part of the strain  $\bar{\boldsymbol{\varepsilon}}$  has a nul term  $\bar{\varepsilon}_{tt}$  which, resorting to the Mohr's Circle concepts, is represented in Figure 5(a). From this, different possibilities for the formation of a strong discontinuity emerge: If the principal strains  $\bar{\varepsilon}_1$  and  $\bar{\varepsilon}_2$  are both positive or both negative (see Figure 5(b)), equation (126) has no solution for  $\mathbf{t}$  and localization is precluded at the considered material point. On the contrary, if  $\bar{\varepsilon}_1 \cdot \bar{\varepsilon}_2 < 0$  two possible planes of discontinuity are provided (see Figure 5(c)). It is worth noting that a unique solution for the discontinuity direction exists only when one of the principal strains is zero, as can be checked from Figure 5(c).

*Uniaxial stress for plane stress cases.* The imposed uniform stress field reads

$$\boldsymbol{\sigma} = \begin{bmatrix} \sigma_{11} & \sigma_{12} \\ \sigma_{12} & \sigma_{22} \end{bmatrix} = \begin{bmatrix} \sigma & 0 \\ 0 & 0 \end{bmatrix} \quad (127)$$

and from the isotropic elastic constitutive equation (24) the regular strain field can be expressed in terms of the Young modulus  $E$  and Poisson's ratio  $\nu$  as

$$\bar{\boldsymbol{\varepsilon}} = \begin{bmatrix} \bar{\varepsilon}_{11} & \bar{\varepsilon}_{12} \\ \bar{\varepsilon}_{12} & \bar{\varepsilon}_{22} \end{bmatrix} = \frac{\sigma}{E} \begin{bmatrix} 1 & 0 \\ 0 & -\nu \end{bmatrix} \quad (128)$$

so that from (128)

$$\bar{\varepsilon}_1 \cdot \bar{\varepsilon}_2 = -\nu \frac{\sigma^2}{E^2} < 0 \quad (129)$$

Thus, two directions exist which can be identified from (42) as:

$$\tan(\theta) = \frac{\pm \sqrt{-\bar{\varepsilon}_{11} \bar{\varepsilon}_{22}}}{\bar{\varepsilon}_{11}} = \pm \sqrt{-\frac{\bar{\varepsilon}_{11}}{\bar{\varepsilon}_{11}}} = \pm \sqrt{\nu} \quad (130)$$

*Uniaxial stress for plane strain cases.* The stress field is given by (127). The strain field is then

$$\bar{\boldsymbol{\varepsilon}} = \begin{bmatrix} \bar{\varepsilon}_{11} & \bar{\varepsilon}_{12} \\ \bar{\varepsilon}_{12} & \bar{\varepsilon}_{22} \end{bmatrix} = \frac{\sigma}{E} \begin{bmatrix} 1 - \nu^2 & 0 \\ 0 & -\nu(1 + \nu) \end{bmatrix} \quad (131)$$

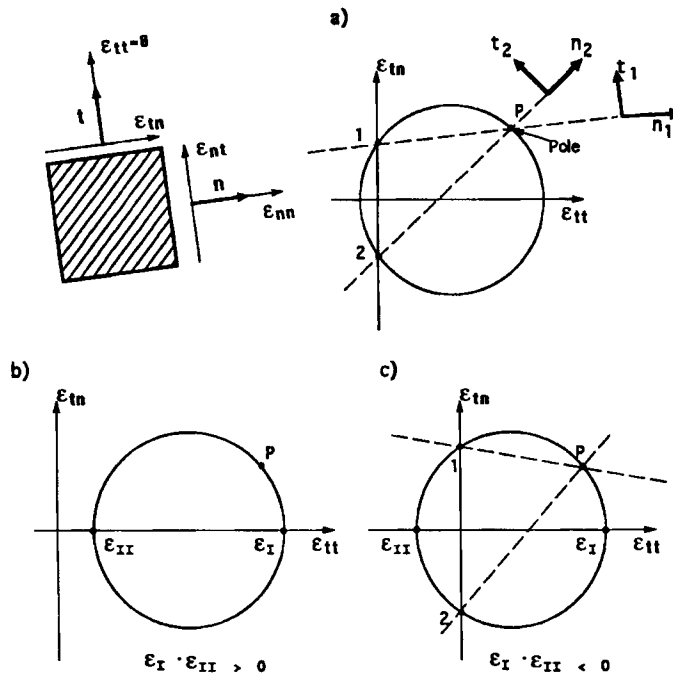


Figure 5. Computation of the discontinuity direction resorting to the Mohr Circle concepts

and thus

$$\bar{\epsilon}_I \cdot \bar{\epsilon}_{II} = -\nu(1 - \nu^2)(1 + \nu) \frac{\sigma^2}{E^2} < 0 \tag{132}$$

Finally,

$$\tan(\theta) = \frac{\pm \sqrt{-\bar{\epsilon}_{11} \bar{\epsilon}_{22}}}{\bar{\epsilon}_{11}} = \pm \sqrt{-\frac{\bar{\epsilon}_{22}}{\bar{\epsilon}_{11}}} = \pm \sqrt{\frac{\nu}{(1 - \nu)}} \tag{133}$$

*Uniaxial strain case.* The imposed strain field is

$$\bar{\epsilon} = \begin{bmatrix} \bar{\epsilon}_{11} & \bar{\epsilon}_{12} \\ \bar{\epsilon}_{12} & \bar{\epsilon}_{22} \end{bmatrix} = \begin{bmatrix} \bar{\epsilon} & 0 \\ 0 & 0 \end{bmatrix} \tag{134}$$

thus,

$$\bar{\epsilon}_I \cdot \bar{\epsilon}_{II} = 0$$

and

$$\tan(\theta) = \pm \sqrt{-\frac{\bar{\epsilon}_{22}}{\bar{\epsilon}_{11}}} = 0 \tag{135}$$

and only one solution ( $\theta = 0$ ) for the direction of the discontinuity exists.

*III.1.2. J2 flow theory.* For J2 flow theory cases it can be shown (see Appendix II, Section II.1.3) that the deviatoric stress components in the Cartesian axes defined by  $\mathbf{n}$  and  $\mathbf{t}$  are given by

$$\mathbf{S} = \begin{bmatrix} S_{nn} & \sigma_{nt} \\ \sigma_{nt} & S_{tt} \end{bmatrix}_s = \begin{bmatrix} 0 & \tau \\ \tau & 0 \end{bmatrix}_s \tag{136}$$



so that a *pure shear* deviatoric stress state, appears at the discontinuity line  $\mathcal{S}$ . From (136) immediately emerges that the inclination angle of  $\mathbf{n}$  with respect to the maximum principal deviatoric stress at  $\mathcal{S}$  is given by

$$\theta = \pm \frac{\pi}{4} \tag{137}$$

Since the principal directions of the stress and the deviatoric stress tensors are the same, (137) also holds for the complete stress tensor. This result was also stated in Reference [17].

The existence of a pure shear deviatoric stress state at  $\mathcal{S}$ , as necessary condition for the appearance of an slip line in plane strain conditions, and (137), can also be established from the analysis of the singularity of the acoustic tensor in (see, for instance, References [20] and [21]). However, it has to be emphasized that, in the context of the strong discontinuity analysis, these conditions are derived from the stress field at the slip line ( $\sigma_{\mathcal{S}}$ ) and *do not apply to the stress field at the continuous part* ( $\sigma_{\Omega \setminus \mathcal{S}}$ ) (since the stress field is not necessarily continuous across  $\mathcal{S}$  at the initiation time  $\implies \sigma_{\mathcal{S}} \neq \sigma_{\Omega \setminus \mathcal{S}}$ )

On the other hand, the localization condition and the inclination angle can be derived in terms of  $\sigma_{\Omega \setminus \mathcal{S}}$ , taking advantage of the condition  $S_{nn|_{\Omega \setminus \mathcal{S}}} = 0$  (see Appendix II, equation (125)) at the initiation time. In fact, this condition can be written, in terms of the principal deviatoric stresses ( $S_{1|\Omega \setminus \mathcal{S}}$  and  $S_{2|\Omega \setminus \mathcal{S}}$ ) and the angle  $\bar{\theta}$  formed by  $\mathbf{n}$  with  $S_{1|\Omega \setminus \mathcal{S}}$ , as

$$\left[ S_{1|\Omega \setminus \mathcal{S}} \cos^2 \bar{\theta} + S_{2|\Omega \setminus \mathcal{S}} \sin^2 \bar{\theta} \right]_{\mathbf{x} \in \mathcal{S}} = 0 \tag{138}$$

In order to have real solutions for  $\bar{\theta}$ , equation (138) states the different sign of  $S_{1|\Omega \setminus \mathcal{S}}$  and  $S_{2|\Omega \setminus \mathcal{S}}$  ( $S_{1|\Omega \setminus \mathcal{S}} \cdot S_{2|\Omega \setminus \mathcal{S}} \leq 0$ ) as necessary condition for the appearance of the slip line, and provides two possible solutions of  $\bar{\theta}$  given by

$$\tan^2 \bar{\theta} = - \frac{S_{1|\Omega \setminus \mathcal{S}}}{S_{2|\Omega \setminus \mathcal{S}}} \Big|_{\mathbf{x} \in \mathcal{S}} \tag{139}$$

As a matter of example, for the case of an uniaxial in-plane stress state given by  $\sigma_{11} = \sigma, \sigma_{22} = \sigma_{23} = 0, \sigma_{33} = \nu \sigma$ , we find,  $S_1 = (2 - \nu)/3, S_2 = -(1 + \nu)/3$  and then, from (139), we obtain

$$\tan^2 \bar{\theta} = \frac{2 - \nu}{1 + \nu} \tag{140}$$

Finally, for the particular case of elastic incompressibility ( $\nu = 0.5$ ), the inclination angle of  $\mathbf{n}$ , with respect to  $\sigma_{11}$ , given by (140) is  $\bar{\theta} = \pm \pi/4$ .

REFERENCES

1. R. Hill, 'Acceleration waves in solids', *J. Mech. Phys. Solids*, **16**, 1-10 (1962).
2. E. N. Dvorkin, A. M. Cuitiño and G. Gioia 'Finite elements with displacement interpolated embedded localization lines insensitive to mesh size and distortions'; *Int. j. numer. methods eng.*, **30**, 541-564, (1990).
3. A. Hillerborg, 'Numerical methods to simulate softening and fracture of concrete', in: G.C. Sih and A. Di Tomaso (eds.), *Fracture Mechanics of Concrete: Structural Application and Numerical Calculation*, 1985, pp. 141-170.
4. H. R. Lofti and P. B. Shing, 'Analysis of concrete fracture with an embedded crack approach'. in: H. Mang *et al.* (eds.), *Proc. EURO-C 1994 Computer Modelling of Concrete Structures*, Pineridge Press, Swansea, 1994, 343-352.
5. T. Belytschko, J. Fish and B. E. Engelmann, 'A finite element with embedded localization zones'. *Comput. Methods Appl. Mech. Eng.*, **70**, 59-89, (1988).
6. J. Oliver, 'A consistent characteristic length for smeared cracking models', *Int. j. numer. methods eng.*, **28**, 461-474 (1989).
7. J. Oliver, M. Cervera, S. Oller and J. Lubliner, 'Isotropic damage models and smeared crack analysis of concrete', in: N. Bicanic *et al.* (eds.), *Proc. SCI-C Computer Aided Analysis and Design of Concrete Structures*, Pineridge Press, Swansea, 1990, pp. 945-951.
8. O. C. Zienkiewicz, M. Huang and M. Pastor, 'Localization problems in plasticity using finite elements with adaptive remeshing'; *Int. j. numer. methods eng.*, **19**, 127-148 (1995).

9. G. Pijaudier Cabot and Z. P. Bazant, 'Nonlocal damage theory', *J. Eng. Mech. ASCE*, **113**, 1512–1533 (1987).
10. R. De Borst, H. B. Muhlhaus, J. Pamin and L. J. Sluys 'Computational modelling of localisation of deformation, in D. R. J. Owen *et al.*, (eds.), *Proc. 3rd Conf. on Computational Plasticity: Fundamentals and Applications*, Pineridge Press, Swansea, 1992, pp. 483–508.
11. A. Needleman, 'Material rate dependence and mesh sensitivity in localization problems', *Comput. Methods. Appl. Mech. Eng.*, **67**, 69–86 (1988).
12. J. C. Simo, J. Oliver and F. Armero, 'An analysis of strong discontinuities induced by strain-softening in rate-independent inelastic solids', *Comput. Mech.*, **12**, 277–296 (1993).
13. J. Oliver and J. C. Simo, 'Modelling strong discontinuities by means of strain softening constitutive equations', in: H. Mang *et al.* (eds.), *Proc. EURO-C 1994 Computer Modelling of Concrete Structures*, Pineridge Press, Swansea, 1994, pp. 363–372.
14. J. C. Simo and J. Oliver, 'A new approach to the analysis and simulation of strong discontinuities', in: Z. P. Bazant *et al.*, (eds.), *Fracture and Damage in Quasibrittle Structures*, E & FN Spon, 1994, pp. 25–39.
15. J. Oliver, 'Continuum modelling of strong discontinuities in solid mechanics', in: D. R. J. Owen *et al.* (eds.), *Proc. COMPLAS IV, 4th Int. Conf. on Computational Plasticity*, Pineridge Press, Swansea, 1995, pp. 455–479.
16. R. Larsson, K. Runesson and M. Akesson 'Embedded localization band based on regularized strong discontinuity', in D. R. J. Owen *et al.* (eds.), *Proc. COMPLAS IV, 4th Int. Conf. on Computational Plasticity*, Pineridge Press, Swansea, 1995, pp. 599–610.
17. F. Armero and K. Garikipati, 'Recent advances in the analysis and numerical simulation of strain localization in inelastic solids', D. R. J. Owen *et al.*, (eds.), *Proc. COMPLAS IV 4th Int. Conf. on Computational Plasticity*, Pineridge Press, Swansea, 1995, pp. 547–561.
18. K. Willam and N. Sobh, 'Bifurcation analysis of tangential material operators', in: G. N. Pande *et al.* (eds.), *Proc. NUMETA-87 Transient/Dynamic Analysis of Constitutive Laws for Engineering Materials*, C4/1-C4/13, Martinus Nijhoff Publishers, Dordrecht, 1987.
19. N. S. Ottosen and K. Runesson, 'Properties of discontinuous bifurcation solutions in elasto-plasticity', *Int. J. Solids Struct.*, **27**, 401–421, (1991).
20. R. Larsson, K. Runesson and N. S. Ottosen 'Discontinuous displacement approximation for capturing plastic localization; *Int. j. numer. methods eng.*, **36**, 2087–2105, (1993).
21. K. Runesson, N. S. Ottosen and D. Peric, 'Discontinuous bifurcations of elastic-plastic solutions at plane stress and plane strain', *Int. J. Plasticity*, **7**, 99–121 (1991).